

HUBBLE SPACE TELESCOPE IMAGING OF the CFRS and LDSS REDSHIFT SURVEYS— III. Field elliptical galaxies at $0.2 < z < 1.0$ ^{1,2}

David Schade^a, S.J. Lilly^b, D. Crampton^a, R. S. Ellis^c, O. Le Fèvre^{d,e}, Francois Hammer^e, Jarle Brinchmann^c, R. Abraham^c, Matthew Colless^f, K. Glazebrook^g, L. Tresse^c, Tom Broadhurstⁱ

^a*National Research Council Canada, HIA/DAO, 5071 West Saanich Road, Victoria V8X 4M6, Canada*

^b*Dept. of Astronomy, University of Toronto, 60 St. George St., Toronto M5S 3H8, Canada*

^c*Institute of Astronomy, Madingley Road, CB3 0HA Cambridge, England*

^d*Laboratoire d'Astronomie Spatiale, Traverse du Siphon, B.P.S. 13376 Marseille, Cedex 12, France*

^e*Observatoire de Paris, Section de Meudon, DAEC, 92195 Meudon Principal Cedex, France*

^f*Research School of Astronomy and Astrophysics, Australian National University, Canberra, ACT 0200, Australia*

^g*Anglo-Australian Observatory, Siding Spring, Coonabarabran, NSW 2357, Australia*

ⁱ*Astronomy Department, University of California, Berkeley, CA 94720, USA*

ABSTRACT

Two-dimensional surface photometry has been performed on a magnitude-limited sample of 46 field galaxies that are classified as ellipticals based on two-dimensional fitting of their luminosity profiles using Hubble Space Telescope imaging. These galaxies are described well by a deVaucouleurs $R^{1/4}$ profile. The sample was selected from the combined Canada-France and LDSS redshift surveys and spans the redshift range $0.20 < z < 1.00$. This analysis reveals several clear evolutionary trends. First, the relationship between galaxy half-light radius and luminosity evolves with redshift such that a galaxy of a given size is more luminous by $\Delta M_B = -0.97 \pm 0.14$ mag at $z = 0.92$ relative to the local cluster elliptical relation. Second, the mean rest-frame color shifts blueward with redshift by $\Delta(U - V) = -0.68 \pm 0.11$ at $z = 0.92$ relative to the same relation in the Coma cluster. These shifts in color and luminosity of field elliptical galaxies are similar to those measured for cluster ellipticals. Approximately 1/3 of these elliptical galaxies (independent of redshift) exhibit [OII] 3727 emission lines with equivalent widths > 15 angstroms indicating ongoing star formation. Therefore, field elliptical galaxies are not composed entirely of very old stellar populations. Estimated star-formation rates together with stellar population evolutionary models imply that $\leq 5\%$ of the stellar mass in the elliptical galaxy population has been formed since $z = 1$. We find some evidence that the dispersion in color among field ellipticals at $z \sim 0.55$ may be larger than that seen among samples of cluster ellipticals and S0 galaxies at similar redshift. We see no evidence for a decline in the space density of early-type galaxies with look-back time. The $\langle V/V_{max} \rangle$ statistics and a comparison with local luminosity functions are both consistent with the view that the population of massive early-type galaxies was largely

¹Based on observations with the NASA/ESA *Hubble Space Telescope* obtained at the Space Telescope Science Institute, which is operated by the Association of Universities for Research in Astronomy Inc., under NASA contract NAS 5-26555.

²Based in part on data obtained through the facilities of the Canadian Astronomy Data Centre.

in place by $z \sim 1$. This implies that merging is not required since that time to produce the present-day space density of elliptical galaxies. However, the statistics are poor: a larger sample is required to produce a decisive result.

Subject headings: galaxies:evolution—galaxies:fundamental parameters—galaxies:photometry—cosmology: observations

1. INTRODUCTION

The simplest models of galaxy evolution have massive elliptical galaxies forming at high redshift in a rapid collapse and monolithic burst of star formation. Such scenarios have been described by Eggen, Lynden-Bell, & Sandage (1962) and Larson (1975). Thereafter, elliptical galaxy stellar populations age passively, with no further star formation. Hierarchical clustering models (White & Rees 1978, Kauffman, White, & Guiderdoni 1993) require that the most massive objects form at late times via the merging of smaller subunits. In this scenario, massive ellipticals would be assembled recently and would be absent from high-redshift galaxy surveys. At redshift $z = 1$ the space density would be lower a factor of 2-3 (Kauffmann 1996, Baugh, Cole, & Frenk 1996) compared to $z = 0$ for $\Omega_o = 1$ (with a less dramatic decrease expected for smaller Ω_o). These two views of the assembly of massive ellipticals (early monolithic formation and recent merging) are diametrically opposed to one another.

The monolithic collapse/passive evolution scenario will be referred to as the "orthodox" model because of the rigidity of its prohibition of any further star formation following the initial burst at formation. This prohibition renders the color and luminosity evolution that accompany the aging of the galaxy more easily predictable by theoretical means. The late-epoch merging or hierarchical clustering model will be referred to as the "secular" model. It is also useful to define an intermediate or "reform" model which has massive ellipticals assembling most of their stellar mass early (e.g., $z > 3$) but where some fraction of the stars form later ($z < 2$). The reform model is useful both because it represents a plausible physical scenario and because it helps to characterise the sensitivity of different types of observational tests of elliptical galaxy formation and evolution.

In summary, the orthodox and reform models both require the assembly of the majority of the stellar mass of elliptical galaxies at high redshift whereas recent merging plays a central role in elliptical galaxy formation in the secular model.

A large fraction of the work on elliptical galaxies has been concentrated on the cluster environment where early-type galaxies are the dominant population. That work may provide useful insights into the origin and evolution of the field population but those studies might also be misleading if environment plays

a major role in galaxy formation and evolution.

1.1. Evidence in favor of the orthodox view

In many respects, cluster ellipticals appear to form a remarkably homogeneous population. The existence of a well-defined color-luminosity relation for early-type galaxies suggests a degree of homogeneity in that population since color depends on age and metallicity. Bower, Lucey, & Ellis (1992) show that the dispersion in the color-luminosity relation in Coma is small enough to require either a high formation redshift ($z \geq 3$) or a high degree of synchronicity in galaxy formation times.

The existence of a low-scatter fundamental plane for early-type galaxies in clusters (Djorgovski & Davis 1987, Dressler et al. 1987) based on size, surface brightness, and velocity dispersion further implies a degree of regularity in the mass-to-light ratios, and therefore the stellar populations, among the early-type population. Jorgensen, Franx, & Kjaergaard (1996) find no dependence of the fundamental plane coefficients or scatter on environment (e.g., cluster richness or velocity dispersion) a conclusion supported by Pahre, de Carvalho, & Djorgovski (1998). Guzman & Lucey (1993) disagree, suggesting that ellipticals in lower density environments may have slightly younger stellar populations than those residing in regions of higher density. Forbes, Ponman, & Brown (1998) analyse a sample of (mostly field) ellipticals and find a correlation between the time since the last major episode of star formation and fundamental plane residuals. This argues that *field* ellipticals span a wide range in age.

More recently, measurements of the early-type galaxy population have been pushed out to higher redshift. The well-defined color-luminosity relation in clusters at $z = 0.55$ (Ellis et al. 1997) shows that the dispersion among early-type galaxies is small even at that epoch. However, the debate is still active regarding exactly how strong a constraint on elliptical galaxy formation is presented by the colour-magnitude relation (Kauffman & Charlot 1998, Bower, Kodama, & Terlevich 1998).

Studies of the cluster elliptical fundamental plane (van Dokkum & Franx 1996, Kelson et al. 1997, van Dokkum et al. 1998) and the weakening of the Mgb absorption as a function of redshift (Bender, Ziegler, & Bruzual 1996) support simple passively-evolving (orthodox) models. Purely photometric techniques

(Pahre, Djorgovski, & de Carvalho 1996, Barrientos, Schade, & López-Cruz 1996, Schade et al. 1996) have been used to compile larger samples of ellipticals covering a wide range in redshift. Schade, Barrientos & López-Cruz (1997) show that the surface brightness of cluster elliptical galaxies to $z \sim 1$ evolves substantially ($\Delta\mu(B) \sim -1$ mag) in a manner broadly consistent with early-forming and passively-evolving models (e.g., Bruzual & Charlot 1993).

Color evolution of cluster ellipticals (Dressler and Gunn 1990, Aragon-Salamanca et al. 1993, Rakos and Schombert 1995, Oke, Gunn, & Hoessel 1996, Standford, Eisenhardt, & Dickinson 1997) is found to be broadly consistent with passive evolution of an old stellar population with little recent star formation.

Lilly et al. (1995) examined the distributions of $\langle V/V_{max} \rangle$ for a photometrically-defined sample of early-type galaxies (i.e., the subset of red galaxies) in the Canada-France Redshift Survey (CFRS) and found that this population is distributed in space in a manner consistent with a constant space density to $z \sim 1$.

The evidence cited above suggests that "orthodox" models of elliptical galaxy formation provide at least broad agreement with the observed properties of the cluster elliptical population over a range ($z = 0$ to $z \sim 1$) in redshift. In the field, the situation is less well-defined. Sandage & Visvanathan (1978) show that the $z = 0$ field and cluster color-luminosity relations are very similar and have comparably small scatter ($\sigma \simeq 0.10$ mag) implying an evolutionary history that does not depend strongly on environment. Schade et al. (1996) use ground-based imaging to compare cluster and field ellipticals to $z = 0.55$ and find roughly similar amounts of luminosity evolution in the two environments. On the other hand the work by Forbes, Ponman, & Brown (1998) and Guzman & Lucey (1993) suggests evolutionary histories that depend on environment, a result supported by Mobasher & James (1996).

1.2. Evidence against the orthodox view

Observational tests of purely passive evolution come in two flavors. In the first, it is only the orthodox view that can be rejected. That is, the result cannot be used to discriminate between the reform or secular (merging) model. The second flavor constitutes a direct test of the merging model and can provide a rejection of both the orthodox and reform points of

view.

Examples of the first flavor of test are studies that search for high-redshift galaxies that have the colors predicted by population synthesis models for passively-evolving stellar systems. Kauffman, Charlot, & White (1996) claim evidence for strong evolution of the E/S0 population over $0.2 < z < 1.0$ from a V/V_{max} analysis of the Canada-France Redshift Survey (CFRS; Lilly et al. 1995). Selection of a sample of early-type (i.e., E or S0) galaxies was attempted on the basis of optical colors predicted by evolving population synthesis models. Note that Kauffman, Charlot, & White compare the sample selected in this way to the predictions of semi-analytic galaxy formation models for the number density of objects with the *morphological* properties of ellipticals. Their claim of strong evolution requires either that early-type galaxies are absent at high redshift (which would support the secular model) or that they are present but have colors that are blue enough to avoid detection by the particular color selection that was applied to compile the sample. The latter case would support the reform model since the blue color is presumably produced by ongoing star formation.

Totani & Yoshii (1998) have repeated an analysis of the CFRS sample similar to the analysis by Kauffman, Charlot, & White (1996) but do not support the conclusions of the earlier work. In particular, Totani & Yoshii use different evolutionary models to select early-type galaxies and they restrict the sample redshift range to $0.2 < z < 0.8$. The analysis yields results consistent with passive evolution models without merging.

There are other studies searching for high-redshift galaxies with passively-evolving colors. Zepf (1997) concludes from a deep search for objects with very red optical-infrared colors that typical ellipticals must have had significant star formation more recently than $z = 5$. Barger et al. (1998) use infrared observations to estimate that roughly 50% of the local space density of elliptical galaxies was in place with passively-evolving colors at $1.3 < z < 2.2$. Menanteau et al. (1998) conclude that there is a deficit of a factor of 3 or more in the observed number of red ellipticals compared to monolithic collapse models. Abraham et al. (1998) find limited evidence for a diversity of star-formation histories among a sample of 12 bright, morphologically-selected spheroids in the Hubble Deep Field but do not attempt to determine space density variations with redshift.

As has been noted, the observational tests described in the preceding several paragraphs are in principle capable of rejecting only the orthodox model even if the experiments are perfectly executed. In other words, they may fail to detect the expected number of galaxies at high redshift because either a) the galaxies are absent (because they form via merging at an epoch later than the epoch of observation) or b) the galaxies are present but bluer than the threshold color. These experiments rely on theoretical models to predict the expected colors. Therefore, actual galaxies may be bluer than the theoretical threshold because they have undergone recent star formation (and thus violate the tenets of the orthodox model) or because the theoretical colors for passively-evolving populations are in error. For example, Jimenez et al. (1998) present an alternative model for the evolution of a stellar population where more than 90% of the stellar mass of ellipticals is formed in the first gigayear of their existence yet these galaxies are substantially bluer than standard population synthesis models at intermediate redshifts. This study illustrates that uncertainties in modelling old stellar populations may be a significant contributor to uncertainties in the conclusions drawn from searches for very red galaxies at intermediate redshifts.

1.3. Evidence in favor of the merging scenario

Theories based on hierarchical cluster models of structure formation (e.g. White & Rees 1978) naturally predict that massive galaxies will be the last galaxies to form by merging. Numerical simulations of disk-disk mergers (White & Negroponte 1973, Barnes & Hernquist 1996) showing that the remnants have a number of properties similar to elliptical galaxies give this scenario further plausibility. On the observational side, studies of close pairs of galaxies (Zepf & Koo 1989, Carlberg, Pritchet, & Infante 1994, Patton et al. 1997) indicate that the galaxy interaction or merging rate rises steeply with redshift ($\sim (1+z)^3$). This result is supported by a study of the pair fractions and merging rate in the CFRS sample (Le Fèvre et al. 1999).

Schweizer & Seitzer (1992) studied the relation between morphological features and colors among local early-type galaxies. They find evidence that the colors of field and group E and S0 galaxies are correlated with the presence of fine morphological structure believed to be produced by merging events. They argue that the systematic shift toward bluer colors with

increased structure is likely produced by systematic variations in the mean age of the stellar population. The elapsed times since the last merger events are estimated to be in the 3-10 Gyr range.

The elliptical galaxy population contains many examples of galaxy cores that are kinematically decoupled from the main body of the galaxy (Bender 1992 and references therein). Although this is clearly evidence against monolithic formation of the entire stellar population in ellipticals, it is not clear whether it requires major mergers or whether more minor interactions might be responsible (see, e.g., Hau & Thompson 1994).

At high redshift there are tests that bypass color information (and thus bypass the uncertainties in the population synthesis models) by selecting early-type galaxies directly on the basis of morphology.

Counts of galaxies as a function of morphological type (Driver et al. 1998) in the the Hubble Deep Field (HDF) provide an indication at roughly the 2σ level of a deficit of elliptical galaxies at $z > 1$ relative to purely passively-evolving models. Franceschini et al. (1998) use a K-band selected sample together with morphological information to define a sample of 35 elliptical and S0 galaxies in the HDF with spectroscopic or photometric redshifts. These authors suggest that the episodes of star formation that produce field ellipticals are spread over a wide range in redshift ($1 < z < 4$) rather than concentrated in a single burst at any epoch (a similar result is found by Kodama, Bower, & Bell 1998). They also note a deficit of early-type galaxies at $z > 1.3$.

The HDF samples are small and originate in a single small field and are so are susceptible to the effects of clustering along the line of sight.³ Clearly multiple lines of sight offer distinct advantages.

1.4. Evidence against the merging scenario

In an attempt to confirm the results of Schweizer & Seitzer (1992), Silva & Bothun (1998a) used near-

³As a check on this problem a subsample matching the selection criteria of the CFRS sample ($I_{AB} \leq 22.5$) can be extracted from the Franceschini et al. sample. Depending on the morphology classification chosen (including or excluding S0s) and the assumed redshift of completeness for the CFRS ($z = 0.8$ or $z = 1.0$) the ratio of Franceschini to CFRS early-type galaxies per unit area is in the range 2.2 to 2.9 indicating a significant surplus of early-type galaxies with $I_{AB} \leq 22.5$ in the HDF (relative to the CFRS which is averaged over many lines of sight) up to $z = 1$.

infrared imaging to search for an intermediate-age (1-3 Gyr) stellar population among a sample of ellipticals with morphological signatures of mergers (largely overlapping the Schweizer & Seitzer sample). They find that these galaxies cannot be distinguished from those ellipticals without signs of interaction and that a small fraction ($< 15\%$ at most) of the stellar mass can be attributed to an intermediate-age population. The test is based on the search for an intermediate-age asymptotic giant-branch population. The search for evidence of mergers is extended (Silva & Bothun 1998b) into the central regions of the galaxies where gas-rich disk-disk mergers would be expected to produce a concentration of younger stars but no compelling evidence for such a population is found. These authors argue that any merging that has occurred has not been accompanied by a strong burst of star formation, either distributed globally or concentrated in the central regions of the galaxies.

A measurement of the space density of large ellipticals as a function of look-back time could produce a direct resolution to the issue of merging as an important process in forming elliptical galaxies. Density evolution can be detected using either the V/V_{max} statistic (which tests the hypothesis that a population is distributed uniformly in distance) or by direct comparison of estimated space densities of large ellipticals at high and low redshift. If merging is important for producing early-type galaxies then there must be fewer large elliptical galaxies at high redshift and a correspondingly low value of the $\langle V/V_{max} \rangle$ statistic.

In a key piece of work Im et al. (1996) construct the luminosity function (LF) for a sample of 376 E/S0 galaxies selected by morphology and luminosity-profile analysis but *independent of color*. They use HST imaging and photometric redshifts based on a training set of their own and CFRS redshifts and detect evolution in the characteristic luminosity of the early-type LF. They find a value of $\langle V/V_{max} \rangle = 0.58 \pm 0.01$ for their entire sample. Note that the high value of $\langle V/V_{max} \rangle$ implies an excess probability of finding ellipticals at high redshift. Presumably this excess is produced by the positive luminosity evolution rather than by an increase in space density. A correction for that evolution would reduce $\langle V/V_{max} \rangle$. The value of $\langle V/V_{max} \rangle$ and the form of the luminosity function are both consistent with a constant space density of elliptical galaxies to $z \sim 1$. The great strength of this study lies in the

large number of galaxies used which provides a firm statistical footing but the weakness lies in the small numbers of spectroscopic redshifts used as a training set for the redshifts based on $V - I$ color, apparent magnitude, and half-light radius.

In summary, there are strong theoretical reasons to believe that recent merging may be an important process governing the assembly of massive galaxies. Much of the evidence that very red (i.e. old and passively-evolving) galaxies are deficient in space density at high redshift are based upon small samples so that the statistical uncertainty is large. In addition there is uncertainty in the theoretical models used to define the color threshold for the sample selection. In any case, studies based on color selection cannot discriminate between the secular (merging) and reform models so they do not provide direct support for the merging scenario. Comparisons of morphologically selected samples (number counts or luminosity functions) disagree with one another. However, the Im et al. (1996) is a strong piece of evidence that the space density of large ellipticals has changed little since $z = 1$.

1.5. The present study

The definition of an elliptical galaxy used throughout this paper is based on two-dimensional fitting procedures and is independent of color. Only those galaxies that are well-fit by an $R^{1/4}$ profile (de Vaucouleurs 1948) with no significant evidence of an additional disk component are used. Those with asymmetry index greater than 0.10 (Schade et al. 1995; roughly the fraction of the total flux contained in the asymmetric component of the galaxy within 5 kpc of the galaxy center) have been excluded.

This is the third of a series of four papers based on an amalgamation of redshifts and HST imaging for galaxies in the Canada-France Redshift Survey (Lilly et al. 1995a and references therein) and LDSS Redshift Survey (Ellis et al. 1996). The series forms a comprehensive study of the evolution of galaxy populations to $z = 1$ using a complete sample of 341 galaxies with HST imaging. Brinchmann et al. (1998) (hereafter referred to as Paper I) discuss the morphological properties of the sample as a whole and Lilly et al. (1998) (hereafter referred to as Paper II) discuss the quantitative morphologies of the late-type population. Le Fèvre et al. (1998) (Paper IV) deals with the merging history of luminous galaxies.

The present paper discusses the galaxy sample and the image processing procedures (§2), results for elliptical galaxies are presented in §3 and are discussed in §4. Throughout this paper (unless otherwise noted) we have adopted $H_0 = 50h_{50} \text{ km sec}^{-1} \text{ Mpc}^{-1}$ and $q_0 = 0.5$.

2. DATA AND PROCEDURE

2.1. CFRS/LDSS Imaging

Details of the sample selection and imaging data are given in Paper I and are summarised here. HST imaging was obtained for a sample of 341 galaxies from the combined Canada-France Redshift Survey with a limiting magnitude of $I_{AB} = 22.5$ and the LDSS Redshift Survey (limit $b_j = 24$, Ellis et al. 1996) datasets. Typical exposures were 6300 seconds in the F814W filter. A subset of the fields also had F450W images of 6300 seconds duration. Archival images in F814W and F606W (typically 4500 seconds) from the region where the CFRS overlaps the ‘‘Groth strip’’ were also used. These overlaps provided multiple images for 38 galaxies. The typical signal-to-noise ratio (defined using the total flux within a 3 arcsecond diameter aperture) of the HST imaging is 100 at $I_{AB} = 22$ and this is sufficient to allow visual classification or calculation of concentration index (Paper I) or to allow two-dimensional surface photometry.

2.2. Two-dimensional surface photometry

Given the modest signal-to-noise ratio of the high-redshift galaxy observations, it is appropriate to adopt simple models to characterise the luminosity profile of these galaxies. We adopt models that have been shown to adequately represent the luminosity profiles of most galaxies in the nearby universe (e.g., de Vaucouleurs 1948, Freeman 1970, Kormendy 1977, Kent 1985, Kodaira, Watanabe, & Okamura 1986, van der Kruit 1987, de Jong 1996, Courteau, de Jong, & Broeils 1996). Two-dimensional surface photometry was performed on the HST images via the fitting of two-component parametric models: an exponential disk (Freeman 1970) and $R^{1/4}$ bulge (de Vaucouleurs 1948) (see also de Jong 1996). These models were convolved with an empirically-defined point-spread-function (PSF) and integrated over each pixel of the HST image. Free parameters were size (scale length or half-light radius), axial ratio, and position angle for each component, and fractional bulge luminosity B/T . Together with the galaxy center (as-

sumed to be coincident for the two components) the fits thus require 9 parameters. Fitting was done using a modified Levenberg-Marquardt algorithm (Press et al. 1992). The technique is simple and robust and provides structural and surface brightness information in addition to a morphological classification. The problems of fitting two-component luminosity profiles has been addressed by Simien & de Vaucouleurs (1986) and Schombert & Bothun (1987).

Real galaxies show a large variety of morphological features (bars, dust lanes, spiral structure, companions) and are often asymmetric whereas the models adopted here are idealised and symmetric. In order to deal with these features and also to allow the computation of an asymmetry index, each galaxy was ‘‘symmetrized’’ by the following procedure (see also Elmegreen, B., Elmegreen, D., & Montenegro 1992 and Schade et al. 1995). First, the image of the galaxy was rotated by 180° and subtracted from itself. The resulting ‘‘asymmetric’’ image (with both positive and negative asymmetric pixel values) was clipped so that only positive asymmetries more significant than 2σ remained. This provides an estimate of the asymmetric component of the galaxy image and the difference formed by subtracting this from the original image yields the ‘‘symmetric’’ image. This symmetric image was subjected to the fitting procedure and the ratio of the asymmetric to symmetric flux is taken as an index of the relative importance of the asymmetric component of the galaxy. From a practical standpoint, the symmetric image is free of companions and other problems and results in a much cleaner and reliable fitting process.

Sky background was measured from large areas of the chips and was not a parameter of the fit. Simulations showed that fitting the sky as a free parameter resulted in an increased scatter in the fitted galaxy parameters but did not otherwise effect the results. With the sky held fixed, the models were normalised at each iteration to yield a minimum χ^2 given the current structural parameters.

The fitting process results in measurements for each of the bulge and disk components individually. This allows independent analyses of the evolution of the disk components separately from the galaxy as a whole, or the bulge components in isolation. Perhaps most importantly, the classifications (based solely on fractional bulge luminosity B/T) are independent of color and spectroscopic properties so that no implicit assumptions are made about the stellar populations

in individual galaxies. This approach allows a check of whether spectral energy distribution and morphology are correlated at high redshift and whether that correlation evolves.

A crucial feature of the two-dimensional modelling as a means to measure structural parameters and surface brightnesses is the fact that we have applied these same techniques (Schade, Barrientos & López-Cruz 1997) to nearby elliptical galaxies (albeit in clusters rather than the field) that were observed with similar physical resolution and at similar signal-to-noise ratios. This greatly reduces concerns that some of our trends are due to systematic differences between the analyses of low and high redshift samples.

2.3. Visual examination of the fits

The evaluation of the success of the fitting process and the validity of the model fits was done by a combination of statistics and visual examination of the galaxy, the models, and, most importantly, the residuals. This procedure has subjective elements and needs a clear explanation so that the issue of possible bias can be addressed.

The main function of the visual inspection is to decide whether a single-component or two-component (bulge-plus-disk) model is the best representation of the galaxy under consideration. The smallest reduced χ^2 is not always accepted as the best fit. Two-component models were rejected in favor of single component models if 1) the fitted bulge component was larger and of lower surface brightness than the disk component (this is an explicit bias that we have imposed on the procedure and was the most common type of failure of the fitting process: it occurred in 3% of the galaxies), or 2) the second component was effectively being fitted to low-level residual asymmetries (that escaped the symmetrizing process) in the galaxy rather than a legitimate bulge or disk component (this overlaps with reason 1).

The visual examination relies mainly on the residuals. If an examination of the residuals after the bulge fit has been subtracted shows no evidence for a disk component then the pure bulge fit will be accepted. This is true even if, as happens in some cases, the bulge+disk model fit has a slightly smaller value of χ^2 . This subjective element of the procedure was evaluated by multiple examinations by one of us (DJS) of the fits separated by substantial periods of time. These repeated judgements showed that about 10%

of early-type galaxies drifted from E to S0 or vice versa depending on whether a disk component was considered a plausible. There are 65 early-type (E or S0) galaxies so that the elliptical sample of 46 galaxies may have contamination of about 15%. We adopt this as an estimate of the reliability of our early-type classifications although we will later examine the effect of 25% contamination of the E sample which we consider a limiting case.

2.4. Internal errors from duplicate observations

There exist 38 duplicate galaxy observations. These are independent observations (most being widely separated in time) which were reduced and analysed independently so that they give good estimates of the internal errors of our fitting procedure including potential sources of error such as centroiding, PSF variations, sky subtraction, and the effect of the subjective visual examination procedure.

The results of duplicate fits are shown in Figures 1 and 2. Figure 1 shows B/T , total I magnitude, and the index of asymmetry. Filled symbols represent galaxies with good residuals (symmetric or “normal galaxies”) and open symbols indicate asymmetric galaxies (those with asymmetry index as defined in Schade et al. 1995 of $R > 0.10$). It is important to note that classifications are considered valid only for symmetric galaxies and discussions of evolution of “normal” galaxies in this paper pertains only to those galaxies; asymmetric objects are excluded. The dispersions are indicated on the figures for the *symmetric* galaxies only. The dispersions for the symmetric (and all) galaxies are 0.04 (0.14) for B/T with 70% of the objects having duplicate observations within ± 0.10 . In total magnitude, the dispersion is 0.05 (0.11) magnitudes. The dispersion in the asymmetry index is 0.06. Since the index results in a binary decision (symmetric or asymmetric) it is appropriate to look at the errors in classification. A cutoff of in asymmetry index of 0.10 is adopted here and this results in 5/38 (13%) disagreement between the two classifications, whereas adopting a cutoff of 0.14 in asymmetry index (as adopted by Schade et al. 1995) results in 1/38 (3%) differences in classification. In summary, the repeat observations show that the fitting procedure produces consistent measures of B/T , total magnitude, and asymmetry index, with errors in the range 5-15%.

Figure 2 shows the multiple-fit results for struc-

tural parameters. The dispersions for the symmetric (and asymmetric) disk scale length measurements are 0.04 (0.05) arcseconds, or about 10% for a typical disk, the surface brightness errors are 0.20 (0.46) mag for disks, and the total disk magnitude errors are 0.10 (0.14) mag. The corresponding figures for the bulge (elliptical) measurements are 0.04 (0.04) arcseconds in size, 0.10 (0.14) mag in surface brightness, and 0.04 (0.04) mag in total magnitude.

The duplicate observations are a robust test of the entire analysis process and include all sources of random errors. The size (scale length or half-light radius) and magnitude errors are $\sim 10\%$ as inferred from these comparisons. The surface brightness measurement errors are $\sim 10 - 20\%$.

2.5. Magnitudes and K-corrections

The HST I_{814} magnitudes from the surface photometry were compared to the ground-based CFRS I - band isophotal imaging and the mean difference was -0.006 with a dispersion of 0.35 magnitudes. The k-corrections were calculated according to the procedure given in Lilly et al. (1995). The $(V - I)_{AB}$ color straddles rest-frame B band of $0.2 < z < 0.9$ and the use of observed I -band with an interpolation of the Coleman, Wu, & Weedman spectral energy distributions yields typically small corrections (I -band corresponds to rest-frame B at $z \sim 0.9$) to obtain rest-frame B magnitudes. The B -band surface brightness is derived from the HST F814W observations and the k-corrections and rest-frame $(U - V)_{AB}$ colors are from interpolation of ground based $(V - I)_{AB}$ colors.

2.6. Emission-line measurements

Measurements of the [OII] equivalent width were taken from Table 1 of Hammer et al. (1997 CFRS-XIV) for the CFRS objects, or from the Autofib survey (Ellis et al. 1996), or otherwise were re-measured from the CFRS spectra themselves. The values in our Table 1 are in the observed frame.

2.7. Spectroscopic failures

In the sample of 341 galaxies with HST imaging and spectroscopy there are 18 objects classified morphologically as galaxies where no redshift could be determined from their spectra. These objects were processed along with the galaxies with redshifts. These objects are generally near the magnitude limit of the

survey. The morphology distribution is skewed toward early-type galaxies: 7/18 (40%) are ellipticals compared to 12% Es in the entire sample. This effect is expected because the low frequency of emission lines among early-type galaxies makes redshift determination difficult, particularly at high redshift. The color distribution (see Fig. 5) of the ellipticals without redshifts suggests that most are at $z > 0.5$. Lilly et al. (1995) have derived estimated redshifts for these galaxies using the I_{AB} magnitudes, the $(V - I)_{AB}$ and $(I - K)_{AB}$ colors, and a measure of the compactness of the images and these estimated redshifts are all at $z > 0.6$. These estimated redshifts will be used in some of the analysis that follows.

3. RESULTS

The output from the fitting process consists of a classification (fractional bulge luminosity B/T), size (disk scale length h or bulge half-light radius R_e), surface brightness, and luminosity of each of the bulge and disk components individually. Although colors from HST observations are available for a subset of the galaxies, ground-based $V - I$ colors (Lilly et al 1995, Paper I) are used here to ensure homogeneity.

Table 1 shows the parameters for the sample of CFRS/LDSS galaxies that are classified as ellipticals by the profile-fitting procedure.

3.1. Surface brightness

Figure 3 shows the luminosity-size ($M_B - \log R_e$) relation for those galaxies classified as ellipticals by the fitting and residual examination process. The sample is divided into three slices of redshift and each panel shows the best-fit, fixed-slope, linear fit as a solid line. The dashed line represents the local $M_B - \log R_e$ relation for *cluster* ellipticals ($M_B(AB) = -3.33 \log R_e - 18.65$) derived by Schade, Barrientos, & Lopez-Cruz (1997). As described in that paper the local cluster elliptical relation was determined from ground-based data with similar physical resolution and signal-to-noise ratio to the HST data used here and in that paper. The intention of using such data was to minimise systematic errors between our local fiducial $M_B - \log R_e$ relation and those derived at high redshift which might occur if local data with much higher signal-to-noise ratio and resolution were used.

Galaxies more luminous than $M_B(AB) = -20$ were used to determine the mean shifts of the $M_B - \log R_e$ locus with “discrepant” points included and

excluded. “Discrepant” points are defined as those where the visual classification given in Paper I was Sab or later thus presenting an apparent conflict with the classifications presented here based on model fits. Duplicate observations for galaxies are treated as independent points but results are also calculated excluding them. The shifts were estimated by minimising the residuals in magnitude (minimising the size residuals was also tried and the difference in the results was negligible) while holding the slope of the linear relation fixed at the value found by Schade, Barrientos, & Lopez-Cruz (1997). The estimated shifts in luminosity are given in Table 2.

There is significant evolution in the $M_B - \log R_e$ relation although there is substantial scatter in the relation, particularly in the interval $0.5 < z < 0.75$. Figure 3 uses symbols coded to indicate discrepant points (defined above) and galaxies with measurable [OII] 3727 emission lines.

Elliptical galaxies with strong [OII] emission (indicating star-formation) might be expected to be over-luminous relative to passively-evolving galaxies if a normal initial-mass function is assumed. In the absence of that assumption it is possible that a small number of massive, UV-bright stars could drive the [OII] emission and blue colors without significantly enhancing the luminosity. The observations show that they are roughly equally distributed on both sides of the mean $M_B - \log R_e$ relation: no luminosity enhancement is seen. The substantial scatter might mask the expected effect but this issue needs further investigation with a larger sample.

We have also examined what effect would be produced if S0 galaxies are mis-classified as ellipticals. Such objects would preferentially lie to the right of the mean $M_B - \log R_e$ relation because their disks would cause the bulge half-light radius to be fit too large (this assumes that their bulges conform to the passive-evolution model appropriate to the ellipticals). This is not seen in the data. The conclusion is that none of these classes of objects ([OII]-strong, discrepant, possible mis-classified S0s) is an important causal factor in the observed shifts in the $M_B - \log R_e$ relations.

We treat spectroscopic failures by adopting their photometrically-estimated redshift, plotting them on Figure 3 as stars, and indicating the trajectories they would follow as a function of redshifts (from $z = 0.2$ to $z = 1.0$).

The amount of evolution in the size-luminosity relation is consistent with what is expected from passively evolving models of old stellar populations (e.g., Bruzual & Charlot 1993) for reasonable values of the initial stellar mass function if the population is sufficiently old.

3.2. Colors

Figure 4 shows the color-luminosity relations for CFRS field ellipticals (we exclude LDSS galaxies because they were observed in a different color system) in three redshift slices. We compute rest-frame $(U - V)_{AB}$ as outlined in §2.5. The dotted line (which coincides with the solid line in the low-redshift panel) is the adopted local relation from Bower, Lucey, & Ellis (1992) for Coma assuming a redshift of 0.0232 so that $(m - M)_V = 35.73$ and $(B - V) = 0.96$ for ellipticals. Noting that $(U - V)_{AB} = (U - V) + 0.7$ and that $B_{AB} = B - 0.17$ yields a Coma relation $(U - V)_{AB} = -0.079M_{AB}(B) + 0.51$. The colors of the ellipticals with $0.2 < z < 0.5$ in Figure 4 agree very well with the Coma relation.

In the following process we have assumed that the observed colors of field ellipticals can be represented by a linear relation with the same slope as the local *cluster* relation (given above) modified only by a uniform shift in color. In fact, a Spearman rank correlation test does not provide significant evidence of the existence of a correlation between color and magnitude for the data in Figure 4 but this is not surprising given the errors and the shallowness of the slope of the color-magnitude relation.

The shifts in the color-luminosity relation are computed holding the slope fixed and minimising the χ^2 residuals in $(U - V)$. Note that the errors in color (derived from ground-based $(V - I)_{AB}$ measurements) and luminosity (from HST measurements) are independent except to the extent that $(V - I)_{AB}$ was used to compute the K-corrections. The results are given in Table 3 and the mean shifts are shown as solid lines in Figure 4. Note that the shift $(U - V)$ for an actual galaxy requires a correction if that galaxy evolves in luminosity as well as color. For luminosity evolution of ΔM_B and an observed color shift of $\Delta(U - V)$ a correction of $\frac{d(U - V)}{dM} \times \Delta M$ is needed in the sense that a physical galaxy undergoes a smaller blueward shift. Table 3 shifts are not corrected for this effect.

Ellis et al. (1997) study the color-luminosity relation for cluster E/S0 galaxies at $z \sim 0.55$. At this

redshift the $V_{555} - I_{814}$ colors approximate restframe ($U - V$). The observed mean color-luminosity relation for 3 clusters is shifted blueward by $\simeq -0.3$ mag in $V_{555} - I_{814}$ which is consistent with the luminosity evolution-corrected shift of $\Delta(U - V) = -0.26 \pm 0.08$ at $z(\text{median}) = 0.59$ for field ellipticals measured here. At higher redshifts, Stanford, Eisenhardt, & Dickinson (1998) estimate the shift in U-infrared color to be $\simeq -0.4 - 0.6$ mag at $z = 0.8 - 0.9$ for a sample of cluster early-type galaxies and we estimate a shift of $\Delta(U - V) \simeq -0.4 - 0.6$ mag from Figure 1 of Kodama, Bower, & Bell (1998) for early-type galaxies in the Hubble Deep Field. Our value of $\Delta(U - V) = -0.68 \pm 0.11$ is consistent with those values.

An examination of the coded symbols on Figure 4 does not suggest that the shift in mean color is produced by any of the sub-populations, e.g., galaxies with [OII] emission, discrepant galaxies, or spectroscopic failures. Although there is a hint that the ellipticals with measurable [OII] emission are bluer than those without [OII], the distributions in color of the two populations cannot be distinguished by a Kolmogorov-Smirnoff test.

A second quantity of interest, in addition to the shift in color, is the dispersion in color (σ) at each redshift. The observed dispersion is a combination of the intrinsic dispersion in the color-magnitude relation and the measurement errors. We remove the contribution from the measurement errors using a procedure from Statistical Consulting Center for Astronomy at Pennsylvania State University (see also Akritas & Bershady 1996). The observations are denoted by Y_i and their observational errors by σ_i and the “de-biased” sample variance is given by $N^{-1} \sum (Y_i - \bar{Y})^2 - N^{-1} \sum \sigma_i^2$. An estimate of the variance of the debiased sample variance is $N^{-1} \sum (\xi_i - \bar{\xi})^2$ where $\xi_i = Y_i^2 - \bar{Y}^2 - 2\bar{Y}(Y_i - \bar{Y})$.

The observational errors in $(V - I)_{AB}$ were propagated through the interpolation procedure to obtain the errors in $(U - V)_{AB}$. Given these individual errors we estimate the intrinsic dispersion (and its 1σ error) in the color-luminosity relation is 0.19 ± 0.08 , 0.29 ± 0.11 , and 0.31 ± 0.16 magnitudes in $(U - V)$ in the three redshift slices, respectively. An examination of the HST imaging shows that crowding is not a serious problem for the colors.

The dispersions in color that we find for field ellipticals are larger than the dispersions measured by Bower, Lucey, & Ellis (1992) ($\sigma < 0.06$) in the Virgo

and Coma clusters and by Ellis et al. (1997) in 3 clusters at $z \sim 0.55$. The difference is significant at roughly the 2σ level. Caution requires us to note that a few errors in our classifications might have a large impact on the observed dispersion. In addition, our photometric errors may be slightly underestimated if, for example, the photometric zero points vary slightly from field to field.

On balance we conclude that we have evidence that field ellipticals have a larger color dispersion at a given luminosity than those in clusters, but that the evidence is suggestive rather than conclusive. Kodama, Bower, & Bell (1998) examined the color-magnitude relation for early-type galaxies with spectroscopic or photometric redshifts in the Hubble Deep Field and concluded that half of those galaxies are as old as rich cluster ellipticals. The intrinsic scatter found for those galaxies with $(U - V) > 0.7$ (which is effectively the more luminous part of the sample and is comparable to our own sample) was $\sigma(U - V) = 0.12 \pm 0.06$ compared to our somewhat larger value of 0.31 ± 0.16 at a similar redshift.

3.3. Selection of early-type galaxies: morphology versus color

The central tenet of this paper is that we can reliably isolate a sub-population of galaxies—independent of redshift—with luminosity profiles that fall into a particular class, namely those whose profiles are well-fit by a deVaucouleurs $R^{1/4}$ (with no other component required). For the purposes of this paper we define such galaxies as ellipticals provided, in addition, that they are not strongly asymmetric (asymmetry index $R < 0.10$). These criteria exclude obvious S0 galaxies because they possess disk components. Nevertheless there are borderline cases. The E-S0 boundary is fuzzy.

Figure 5 shows the observed $(V - I)_{AB}$ colors versus redshift for the CFRS sample, with those galaxies classified (from profile fitting) as ellipticals shown as filled circles. The galaxies with fractional bulge luminosity $0.4 < B/T < 1.0$ (loosely called S0s) are indicated by open squares. The majority of the ellipticals are among the reddest galaxies in the sample. What are the other galaxies that are very red? About 1/3 of the red non-ellipticals are classified as S0 galaxies (defined here as galaxies with fractional bulge luminosity $B/T \geq 0.5$), most of the remainder are Sa-Sb galaxies (defined by $0.2 \leq B/T < 0.5$), with a few presumably reddened edge-on disks.

The color distribution of the elliptical sample demonstrates that we are selecting—by morphology alone—a sample of objects with spectral energy distributions that are very different from the average properties of the galaxies in the full sample. This is encouraging. However, the color distribution of ellipticals has large scatter and some disk galaxies are as red as many ellipticals. This is true independent of redshift and thus any color cut to segregate a morphological class appears difficult (perhaps impossible).

Another test of the credibility of our classifications is a comparison with more conventional methods of classification. For this purpose we use the visual classifications given for this dataset in Paper I. In that system the early-type galaxies have classes E=0, E/S0=1, S0=2. Figure 6 shows the observed $(V - I)_{AB}$ versus redshift plot for these galaxies. Filled symbols are those with visual classifications of E/S0 or earlier (numerical visual class ≤ 1 from Paper I). Galaxies with classifications of S0 (visual class 2) are indicated by open squares. The visual classification system and the two-dimensional profile-fitting system yield similar populations in terms of color versus redshift but the dispersion in color for early-type galaxies is large using either method of classification.

There is a fundamental difference in philosophy between selection of a galaxy sub-population by color and selection by morphology. The physical structure of a massive galaxy is more likely to be a stable quantity than is the color of a galaxy. A starburst involving a moderate fraction ($\sim 10\%$) of a galaxy's mass is capable of radically altering the color of the galaxy (albeit temporarily). Such an event is unlikely to have as strong an effect on the apparent structure of the galaxy although admittedly this depends on the spatial distribution and strength of star formation. Morphological selection keys on the apparent structure of the galaxy whereas color selection keys on the current state of the stellar population. This current state depends on the age distribution of its stars and the contemporaneous rate of star-formation (as well as other quantities such as metallicity and the initial mass function). There is also a strong dependence on dust content in the sense that galaxies with young or intermediate-age stellar populations can be shifted into the selection region by reddening.

Kauffman, Charlot, & White (1996) (KCW) have applied a color selection technique to the entire CFRS sample (the present sample is the subset of CFRS galaxies with HST imaging). Details of their evolu-

ing stellar population models are given in that paper. The line plotted on figures 5 and 6 is the selection line (intended to represent the blue edge of the E/S0 population) applied by Kauffman, Charlot, & White (1996) to the CFRS sample. This line is a very poor fit to our morphologically-selected sample but gives us the opportunity to directly compare the morphological and color selection procedures.

Kauffman, Charlot, & White (1996) (hereafter KCW) test the hypothesis that giant ellipticals all formed at high redshift in a brief burst of star formation and that thereafter they evolve passively with no further substantial episodes of star formation. Under this hypothesis the colors and luminosities of those galaxies can be predicted as a function of redshift by modelling the stellar populations. As a practical matter S0 galaxies are lumped together with ellipticals because their colors are similar in the field (Buta et al. 1994) and nearly identical in nearby clusters (Bower, Lucey, & Ellis 1992) and clusters at higher redshift (Ellis et al. 1997). If the stellar models are accurate and the transformation into the observational plane is reliable then all early-forming galaxies with no ongoing star formation can be detected and counted. A comparison can then be made of the space densities of those populations at high and low redshift. If all red galaxies formed long ago ($z \gg 1$) and have since stopped forming stars then the space density will be conserved. If a constant space density is *not* observed then either red galaxies have been created by merging since $z = 1$ or those galaxies are bluer than the selection threshold because of recent star formation.

Figures 5 and 6 show that neither the profile fitting method nor the visual classification yields a sample that corresponds well with that selected by the color criteria of KCW. If a comparison is made with the two-dimensional profile-fitting classification system used in this paper, color selection is both incomplete (success rate of $< 58\%$ for E/S0s) and suffers from contamination (47% of the color-selected sample are not E/S0s but are other red galaxies). Furthermore, the rates of completeness and contamination are a function of redshift. For example, the percentage of ellipticals detected is 57% at $0.2 < z < 0.5$, 36% at $0.5 < z < 0.75$, and 21% at $0.75 < z < 1.0$. The rates of contamination (the fraction of galaxies redder than the threshold that are not E/S0 galaxies) are 56% at $0.2 < z < 0.5$, 22% at $0.5 < z < 0.75$, and 57% at $0.75 < z < 1.0$. Evidently, the selection threshold adopted by KCW does not trace the evolu-

tion of the elliptical galaxy population as it is defined here. Neither does it trace the evolution of the E/S0 population as defined by the visual classification system of Paper I. The difference is attributable to the fact that many of our ellipticals are bluer than the KCW threshold (some have emission lines) and many disk-dominated systems are redder than their threshold. Thus, the claim by Kauffman, Charlot, & White (1996) that they have detected strong evolution in the early-type population is not valid. This point will be addressed in section 3.6 where the V/V_{max} analysis will be repeated using the samples selected here.

Selection by morphology bypasses potential problems with modelling the stellar populations, is affected very little by moderate episodes of star formation, and is not prone to include disk galaxies because of the presence of dust. If the structure of these galaxies is stable then the question is: can a set of morphological criteria be consistently applied over a range of redshift where surface brightness dimming (a $(1+z)^4$ effect) is a strong effect? The most likely error would be failure to detect disks around bright elliptical components at high redshift because of suppression by surface-brightness dimming. At low redshift such a galaxy would be classified as S0. At high redshift such an object would be classified as elliptical. In section 3.6 we will construct samples that address these question of possible errors in the application of the morphological selection.

3.4. Modelling the luminosity and color evolution

For the moment we will ignore the presence of emission lines in these galaxies and compare the evolution in color and luminosity to Isochrone Synthesis Spectral Evolution models (Bruzual & Charlot 1993,1996). The GISSEL95 and GISSEL96 libraries give synthetic colors and luminosities for simple stellar populations (and composite populations) as a function of age with a range of metallicities. The available constraints are the present-day colors of elliptical galaxies (from Buta et al. 1994), together with the evolution in color and luminosity. If we restrict our examination to orthodox models where the entire stellar population of elliptical galaxies is formed in an instantaneous burst, then the available model parameters are the redshift of formation (assumed to be the same for all galaxies), the metal abundance, the stellar initial mass function, and the choice of cosmology. The choice of a particular stellar atlas in GISSEL96 has a negligible effect

on the observables in the present case.

Initially we adopted a Salpeter (1955) initial mass function which has been shown (Charlot & Bruzual 1991, Bruzual & Charlot 1993) to reproduce the colors of local galaxies and we assume solar metallicity unless otherwise noted. We explore only cosmologies with $H_0 = 50 \text{ km sec}^{-1} \text{ Mpc}^{-1}$ and $\lambda = 0$ and use $q_0 = 0.0$ and 0.5 .

If ellipticals were a constant surface brightness population then the derived luminosity evolution would be independent of q_0 . This is not the case. However, the dependence on q_0 is rather weak. At $z = 0.5$ using $q_0 = 0.0$ yields only -0.09 mag more evolution than $q_0 = 0.5$ and at $z = 1$ the effect is -0.18 magnitudes. In the following comparisons, these small corrections necessary for $q_0 = 0$ are applied to the theoretical curves rather than the data. The major effect of varying q_0 is to change the age of the stellar populations for a given formation redshift.

A single-burst population formed at $z = 10$ with $q_0 = 0.5$ is shown plotted on figure 7. The model luminosity evolution from $z = 0$ to $z = 1$ is somewhat larger than observed whereas the model colors are redder than those observed at $z \simeq 0.5$. Note that this plot shows both field and cluster elliptical galaxies from previous work (reduced in a similar manner). The model luminosity evolution can be reduced if $q_0 = 0.0$ (since the population is older) but this makes the $z = 0$ colors much redder and the color evolution is then far too flat. This problem is not relieved by using either of the other initial mass functions (Scalo 1986 or Miller and Scalo 1979) available in these models. Changing the metallicity fails to produce the necessary steeper increase of color with redshift. Since it is likely that the color systems of the models are not identical to the observations, and because of uncertainties in the models themselves (Charlot, Worthey, & Bressan 1996) differences of 2-3 tenths of a magnitude in absolute terms will not be considered a serious disagreement. We choose to give more weight to the comparison of differential effects with redshift.

The observed rapid change with redshift in the mean color of the elliptical galaxy population can be reproduced by lowering the redshift of formation. However, in order to obtain even a reasonable agreement between observed and model color evolution a very recent formation epoch ($z \sim 1.5$) is required and this enhances the luminosity evolution, creating a serious discrepancy. Another way for the models to reproduce the observed color evolution is to superim-

pose bursts of star formation comprised of some fraction of the galaxy mass on top of the old, passively-evolving population. Bursts at $1 < z < 3$ with mass fractions in the range 10-25% are capable of producing the color behavior but they fail to avoid the problem of over-producing luminosity evolution; the same problem as with a more recent, single-burst, formation epoch. A similar difficulty was noted in Hammer et al. (1997) in fitting the 4000 angstrom break of many of the “quiescent” objects with an old, single-burst population.

The fundamental problem is that a change in $(U - V)$ of -0.68 ± 0.11 mag should be accompanied by a much larger brightening (roughly 2 magnitudes in the B band) in a passively evolving system. One particular solution to the modelling problem is to superimpose a small burst of star formation at $z = 1$. A model that fits well is the onset at $z = 1$ of exponentially-declining star formation with an e-folding time of 1 Gyr (a τ model) and a mass of 2.5% of the final stellar mass of the galaxy. Such an effect might be produced by accretion of low-mass companions (see Silva & Bothun 1998a) but precludes a major star-formation episode accompanying a large disk-disk merger. Such a model fits very well if we adopt $q_o = 0$ and a high redshift ($z_f = 10$) of formation of the dominant old population. We show such a model on Figure 7. (Here we have adopted an abundance of 40% solar for the old population and a solar abundance for the star formation starting at $z = 1$. The difference in color at $z = 0$ between the simple models and the two-component models is due mostly to the lower abundance chosen for the old population in these two-component models.) This model is, of course, completely ad hoc. An attempt to provide serious constraints on the modelling process would require accurate mean colors and luminosities for elliptical galaxies over a wide range of redshift.

Nevertheless, it is evidently possible to match the observations presented here with simple models if the dominant stellar population is old (thus the preference for low q_o) in order to match the slope of the luminosity versus age relation but then some more recent ($z \simeq 1$) star formation is required in order to match the strong color evolution. Our estimates of color evolution at $z \simeq 1$ are broadly consistent with both the cluster work of Stanford, Eisenhardt, & Dickinson (1998) and the results for field galaxies by Kodama, Bower, & Bell (1998). However, precise comparisons with the present work are not possible

and we emphasise the uncertainties associated with constraining models with the presently very limited set of observations.

3.5. [OII] Emission and star formation

In the previous section we have ignored the presence of [OII] emission lines which indicate that these galaxies are not composed exclusively of populations formed at $z > 1$. The fraction of galaxies exhibiting strong (equivalent width > 15 angstroms) [OII] is roughly 30% independent of redshift. This compares to $< 3\%$ of a sample of 104 nearby elliptical galaxies (Caldwell 1984). Clearly there has been strong evolution in the emission-line properties of elliptical galaxies since $z = 1$.

We have estimated the star-formation rates (SFRs) for these galaxies using the prescriptions of Kennicutt (1992) using [OII] fluxes or equivalent widths. As emphasised in that paper there are substantial uncertainties in such estimates. The SFRs derived from continuum luminosity coupled with [OII] equivalent width compare very well with those SFRs derived directly from the [OII] fluxes. We have adopted the former method and normalised the SFRs in each redshift bin by the total elliptical galaxy mass in that redshift bin (regardless of [OII] strength). The masses are estimated from the best-fit stellar populations model in the previous section ($q_o = 0.0$, old population plus star formation onset at $z = 1$) which gives B-band luminosity of 8.3 mag per solar mass at $z = 0$. The observed luminosities were corrected to their “de-evolved” luminosities at $z = 0$ to yield masses. Galaxies with photometrically-estimated redshifts were included with [OII] equivalent widths of zero so that they contributed to the mass but not the star-formation rate.

Figure 8 shows the star-formation rate per unit stellar mass in elliptical galaxies as a function of redshift. It is assumed that the SFR is zero for local ellipticals (Kennicutt 1998). If the star-formation were constant from $z = 1$ to the present and remained at the observed high-redshift rate then $\sim 5\%$ of the stellar mass in present-day elliptical galaxies would have formed since $z = 1$. If, instead, the star formation rate is modelled as exponentially declining, a smaller estimated mass fraction results.

3.6. Merging: The density evolution of the early-type population

The present study shows that some level of star formation is maintained in the elliptical population at $z < 1$. Therefore, the "orthodox" model for the formation and evolution of elliptical galaxies is rejected. The remaining (very large) question is the role of late-epoch merging in producing massive ellipticals. The role of merging can be addressed directly by examining the space distribution of a complete sample of these objects. The V/V_{max} statistic (Schmidt 1968, Lilly et al. 1995, Kauffman, Charlot, & White 1996) is one way to address this question. In the case of no evolution V/V_{max} is uniformly distributed between 0 and 1 with a mean of 0.5. The expected 1σ error in the mean of a sample of n objects is $(12n)^{-1/2}$. We have analysed the sample of CFRS ellipticals (excluding LDSS ellipticals in order to produce a homogeneous sample) using this technique and we compare our results with those obtained by Kauffman, Charlot, & White (1996) using the same technique on their color-selected subset of the whole CFRS sample.

Table 4 presents results for the CFRS elliptical sample as well as the early-type sample derived by Brinchmann et al. (1998) in Paper I using visual classification techniques. We compute the mean value of V/V_{max} and the probability (P_{ks}) that the distribution of V/V_{max} is drawn from a uniform parent population (calculated using a Kolmogorov-Smirnov test). This directly represents the probability that a constant-space-density model is acceptable for a specific subsample, cosmology, and assumption about luminosity evolution as indicated in Table 4. We also estimate the exponent γ and its 1σ confidence interval for an evolution law of the functional form $F \propto (1+z)^{-\gamma}$. The value of γ and its error are estimated by varying γ until $V/V_{max} = 0.5 \pm (12n)^{-1/2}$. Luminosity evolution is incorporated into the analysis assuming that $\Delta M_B = -z$ i.e., one magnitude of evolution to $z = 1$. Each galaxy is corrected from its observed luminosity to a redshift-zero fiducial luminosity $M_B(0) = M_B(\text{observed}) + z$. Then its apparent magnitude as a function of redshift is computed from $M_B(z) = M_B(0) - z$ using distance modulus and k-corrections.

We have constructed and analysed the following subsamples. Sample 1 is composed of all elliptical galaxies (as judged from profile fitting) with spectroscopic redshifts. Sample 2 adds spectroscopic failures

adopting their photometric redshifts. In sample 3 we assign all of the spectroscopic failures a redshift of $z = 0.2$. These samples all give results consistent with no evolution at the 95% significance level regardless of cosmology or luminosity evolution.

We address the issue of possible errors in the classifications between E and S0 galaxies (described in the previous section) in two ways. First, from the residuals of the fit we can make some estimate of which ellipticals are most likely to be mis-classified. We adopt what we consider to be an extreme level of contamination (25%) and exclude all of these "possible S0s" from Sample 1. This gives us Sample 4 and the procedure has little effect on the $\langle V/V_{max} \rangle$ results. The second way that we address the classification error problem is to add all S0 galaxies (as judged from profile fitting) to Sample 1 to yield Sample 5. All of these results are consistent with no-evolution models of the population. Note that if we were to add spectroscopic failures at their photometric redshifts we would make $\langle V/V_{max} \rangle$ larger whereas $\langle V/V_{max} \rangle$ needs to be smaller than 0.5 in order to produce the Kauffman, Charlot, & White (1996) result.

An alternative to using the classifications given by the model-fitting approach is to adopt the visual classifications from Paper I. Samples 6 and 7 are constructed using these classifications with and without photometric redshifts, respectively. Sample 6 results in rejection of the no-evolution hypothesis at the 95% significance level for $q_0 = 0.01$. Sample 7 is preferred over sample 6 because it includes spectroscopic failures at their photometrically-estimated redshifts. Sample 7 yields a result consistent with no-evolution models.

The results in Table 4 provide no evidence of evolution in the space density of early-type galaxies regardless of whether that population is defined as elliptical galaxies (by the profile-fitting method) or as E/S0 galaxies using the visual classifications. The most reliable samples in Table 4 are those where photometric redshifts have been adopted where spectroscopic redshifts were not available. These samples are the most reliable because they correct for the expected incompleteness in spectroscopic redshifts for early-type galaxies at high redshift. Considering those "best" samples indicates that no-evolution models are consistent with these datasets independent of cosmology and independent of luminosity evolution.

This conclusion about the evolution of ellipticals from the V/V_{max} statistic contradicts that reached

by Kauffman, Charlot, & White (1996). The color selection method employed in that paper fails to produce a complete, uncontaminated sample of early-type galaxies. Totani & Yoshii (1998) employ their own models to select early-type galaxies on the basis of color. They apply a sample cut-off at $z = 0.8$ based on the assumption that the CFRS is not complete at higher redshifts. With this cut-off they find $\langle V/V_{max} \rangle = 0.478 \pm 0.035$ which is consistent with no evolution.

It is important to appreciate that the size of the error bars allow a factor of 2-3 change in the space density at the 1σ level. Therefore, although the present work provides no evidence for significant evolution in the space density of early-type galaxies *it does not rule out such evolution*. A larger sample would be required to decide the question using a $\langle V/V_{max} \rangle$ test.

Finally, we can compare the observed space density of elliptical galaxies in the CFRS sample to the predictions based on the local luminosity function. For this purpose we use the E/S0 LF of Marzke et al. (1998) (a conversion is required from their $H_o = 100 \text{ km sec}^{-1} \text{ Mpc}^{-1}$ to our value of $H_o = 50 \text{ km sec}^{-1} \text{ Mpc}^{-1}$). The LF is integrated over all galaxies brighter than $M_B(AB) = -20.2$ to yield a space density of $3.47 \times 10^{-3} \text{ Mpc}^{-1}$. The effective area of the HST subsample of the CFRS is taken to be 0.0096 deg^2 . The expected numbers are computed for the three redshift shells $0.2 < z < 0.5$, $0.5 < z < 0.75$, $0.75 < z < 1.0$. In the present case a negligible error is introduced by assuming that each galaxy can be detected throughout is redshift shell and simply multiplying the integral of the luminosity function above by the total volume within the shell, given the area of coverage. We assume that the luminosity evolution of the elliptical population is $M(z) = M(z = 0) - z$ which approximates the results of the present study. Thus we count galaxies in $0.2 < z < 0.5$ brighter than $M_B(AB) = -20.2$, those in $0.5 < z < 0.75$ brighter than -20.7 , and galaxies in $0.75 < z < 1.0$ brighter than $M_B(AB) = -21.2$.

The comparison between observed and predicted numbers are given in Table 5. Because we are comparing classifications derived from visual inspection with those derived from profile-fitting (and at very different redshifts), there is the potential for systematic differences in the populations being counted. On the other hand, we have shown that the visual classifications done on this sample agree broadly with the

profile-fitting classifications. A puzzling feature of the result shown in Table 5 is that we count roughly the same number of elliptical galaxies as are predicted for $q_o = 0.01$ by the LF for elliptical and S0 galaxies combined. Data from Buta et al. (1994) suggests that S0 galaxies will comprise roughly two-thirds of the E/S0 sample whereas the LF's from Marzke et al. 1994 suggest that only one-quarter of an E/S0 sample will consist of ellipticals.

Table 5 provides no evidence for a deficit of elliptical galaxies at high redshift. On the contrary, the problem is that there are more than expected if ellipticals constitute only a fraction (1/3 to 1/4) of the galaxies in the E/S0 luminosity functions used in the calculations. The problem is substantially worse in the case where $q_o = 0.5$. However, if isolated ellipticals gradually accrete halo gas to build a disk (as suggested in some formation scenarios) then these high-redshift ellipticals might evolve into present-day S0 galaxies. An alternative is that we have failed to detect the faint disks around some early-type galaxies at high redshift that would have resulted in a classification of S0 rather than E. Either of these interpretations would result in perfect agreement with the numbers in Table 5 if $q_o \sim 0$.

4. CONCLUSIONS

The analysis of the CFRS/LDSS sample of field elliptical galaxies reveals evolution in the $M_B - \log R_e$ relation so that a galaxy of a given size is more luminous by -0.97 ± 0.14 magnitudes at $z = 0.9$ than its local counterpart as estimated from the cluster elliptical locus. This apparent evolution in luminosity is accompanied by a bluing of these galaxies with look-back time. At $z = 0.9$ the mean shift in color is $-0.68 \pm 0.11 \text{ mag}$ in rest-frame (U-V). The luminosity evolution is consistent with simple models of passive evolution of an old, single-burst stellar population but a small quantity (by mass) of more recent star formation is required to make the models match the observed color evolution. Approximately 1/3 of the elliptical galaxies at $0.2 < z < 1.0$ display [OII] emission lines, indicating star formation at rates that we estimate at $\sim 0.5 M_\odot \text{ yr}^{-1}$ per $10^{11} M_\odot$ of stellar mass in elliptical galaxies so that perhaps a few percent of the stellar populations of these galaxies have formed since $z = 1$.

The estimates of luminosity and color evolution found here are consistent with that found in clusters

(Schade, Barrientos, & López-Cruz 1997, Stanford, Eisenhardt, & Dickinson 1998). On the other hand, we have found evidence that the dispersion in the color-luminosity relation may be larger among field ellipticals at $z > 0.5$ than the dispersion observed for early-type galaxies in Coma by Bower, Lucey, & Ellis (1992) or those in clusters at $z = 0.55$ by Ellis et al. (1997).

The presence of [OII] emission indicates that star formation is occurring in $\sim 30\%$ of the elliptical galaxies in this sample. Thus the "orthodox" view of elliptical galaxy formation (a single burst followed by no further star formation) is false. A larger dispersion in color among field ellipticals than among those in clusters (which is suggested by these data) would also argue in favor of a more diverse star formation history in field ellipticals than in cluster early-type galaxies in the sense that more recent activity occurred in field galaxies possibly because continued gas infall that could fuel ongoing star formation is suppressed in the cluster environment.

We have repeated the $\langle V/V_{max} \rangle$ test for early-type CFRS galaxies done by Kauffman, Charlot, & White (1996) using a subset of the CFRS sample with HST imaging. Our sample was selected on the basis of profile fitting rather than color (the technique they used). We find no evidence for evolution in the space density of large ellipticals over the range $0.2 < z < 1.0$ within the CFRS survey. We cannot rule out fairly large changes (factors $\sim 2-3$) in density because of the small numbers in our survey. Nevertheless, our result contradicts the claim for detection of strong evolution by Kauffman, Charlot, & White (1996) because the color selection applied in that work did not detect all of the E/S0 galaxies that were present and also suffered from contamination by red disk-dominated galaxies.

A more powerful test for a change in space density (although more prone to systematic error because of differences in the classification method) is a comparison of our observed number of field elliptical galaxies at high redshift with the predictions based on the E/S0 luminosity function of Marzke et al. (1998). This test indicates no deficit of early-type galaxies at $z \leq 1$. In fact, there is a surplus of ellipticals at high redshift unless the ratio of E to S0 galaxies increases at high redshift. Such an effect might be spurious. It is plausible that faint disks might be missed at high redshift resulting in mis-classification of S0 galaxies as ellipticals. Alternatively, it might be

a real evolutionary effect where ellipticals are transformed into S0s via the development of disk components. Formally, we can say that, at the 95% confidence level, the number of ellipticals that we detect at $0.75 < z < 1.0$ is between 0.71 and 2.03 times the number of E/S0 galaxies predicted by the Marzke et al. (1998) luminosity function assuming $q_0 = 0.01$ and including spectroscopic failures.

In summary, the results presented here are consistent with an early formation epoch for these elliptical galaxies but with some degree of ongoing star formation at $z < 1$. We reject the orthodox model of elliptical galaxy evolution. We find no evidence that the space density of large ellipticals has changed since $z = 1$. The result of Im et al. (1996) agrees very well with our result and carries substantially more statistical weight. These results directly challenge the view that significant numbers of elliptical galaxies have been formed by mergers since $z = 1$.

A final note on the question of merging. Le Fèvre (1999) find evidence—from the same sample of galaxies studied here—that the rate of bright galaxy mergers increases steeply with redshift. That work suggests that a typical (L^* at $z \sim 1$) galaxy will undergo 1-2 major merging events since $z = 1$. On the other hand, the present study finds no evidence for a significant change in the space density of massive elliptical galaxies since $z = 1$. Furthermore, Lilly et al. (1998) find no significant change in the space density of large disk galaxies over this redshift range. These observations can be reconciled if the enhanced level of interaction and merging that is seen is, in fact, taking place among galaxies that are somewhat less massive than present-day L^* galaxies and if such interactions do not frequently produce large elliptical galaxies.

We acknowledge the support of NATO in the form of a travel grant. The research of SJL was supported by NSERC.

REFERENCES

- Abraham, R., Ellis, R., Fabian, A., Tanvir, N., & Glazebrook, K. 1998 astro-ph 9807140
- Akritas, M. & Bershad, M. 1996 ApJ740, 706
- Aragon-Salamanca, A., Ellis, R., Couch, W., & Carter, D. 1993, MNRAS, 262 764
- Bender, R. 1992 *aj*, 258, 250
- Barger, A., Cowie, L., Trentham, N., Fulton, E., Hu, E., Songaila, A., & Hall, D. 1998 astro-ph 9809299
- Barnes, J. & Hernquist, L. 1996 ApJ, 471, 115
- Barrientos, F., Schade, D., & López-Cruz, O. 1996 ApJ, 460, 89
- Baugh, C., Cole, S., & Frenk, C. 1996 MNRAS283, 1361
- Bender, R., Ziegler, B., & Bruzual, G. 1996, ApJ463, 51
- Bower, R., Kodama, T., & Terlevich, A. 1998, MNRAS, 299, 1193
- Bower, R., Lucey, J., & Ellis, R. 1992 MNRAS254, 601
- Brinchmann, J., Abraham, R., Schade, D., Tresse, L. et al. 1998 ApJ499, 112
- Bruzual, G. & Charlot 1993, ApJ, 405, 538
- Buzzoni, A., 1995, ApJS, 98, 69
- Burstein, D. & Heiles, C. 1982, AJ, 887, 1165
- Buta, R., Mitra, S., deVaucouleurs, G., & Corwin, H. 1994, AJ, 107, 118
- Capelato, H., de Carvalho, R., & Carlberg, R. 1995, ApJ, 451, 525 ApJ, 457, 625
- Carlberg, R., Pritchet, C., & Infante, L. 1994, ApJ, 435, 540
- Charlot, S. & Bruzual, G. 1991, ApJ, 367, 126
- Charlot, S., Worthey, G. & Bressan, A. 1996, ApJ, 457, 625
- Coleman, G., Wu, C. & Weedman, D. 1980, ApJS, 43, 393
- Crampton, D., LeFèvre, O., Lilly, S., & Hammer, F. 1995, ApJ, 455, 96
- de Carvalho, R., & Djorgovski, S., 1992, ApJ, 389, 49
- Dickinson, M. 1995 in *Fresh Views of Elliptical Galaxies*, A.S.P. Conference Series, ed. Buzzoni, A., Renzini, A., & Serrano, A. p. 283
- van Dokkum, P., Franx, M., Kelson, D., & Illingworth, G. 1996, ApJ, 504, L17
- van Dokkum, P. & Franx, M. 1996, MNRAS, 281, 985
- Djorgovski, S., & Davis, M. 1987, ApJ, 313 59
- Dressler, A., Lynden-Bell, D., Burstein, D., Davies, R., Faber, S., Terlevich, R., Wegner, G. 1987, ApJ, 313, 42
- Dressler, A., & Gunn, J. 1990, in *Evolution of the universe of galaxies*, San Francisco, Astronomical Society of the Pacific
- Driver, S., Windhorst, R., Phillips, S., & Bristow, P. 1996, ApJ, 525, 533
- Driver, S., Fernandez-Soto, A., Couch, W., Odewahn, S., Windhorst, R., Phillips, S., Lanzetta, K., & Yahil, A. 1998 ApJ, 496, 93
- Eggen, O., Lynden-Bell, D., & Sandage, A., 1962 ApJ, 136, 748
- Ellis, R., Smail, I., Dressler, A., Couch, W., Oemler, A., Butcher, H., & Sharples, R. 1997 ApJ, 483, 582
- Ellis, R., Colless, M., Broadhurst, T., Heyl, J., & Glazebrook, K. 1996, MNRAS, 280, 235
- Elmegreen, B., Elmegreen, D., & Montenegro, L. 1992, ApJS, 79, 37
- Feigelson, E., & Babu, G. 1992 ApJ, 397, 55
- Forbes, D., Ponman, T. & Brown, R. 1998 ApJ, 508, 43
- Franceschini, A., Silva, L., Fasano, G., Granato, G., Bressan, A., Arnouts, S., & Danese, L. 1998, ApJ, 506, 600
- Freeman, K. 1970 ApJ160, 811
- Guzman, R., & Lucey, J. 1993 MNRAS263, 47
- Hammer, F. et al. 1997, ApJ, 481, 49
- Hau, G. & Thompson, R. 1994 MNRAS270, 23
- Im, M., Griffiths, R., Ratnatunga, K., Sarajedini, V. 1996, ApJ, 461, 79
- de Jong, R. 1996 A&AS, 118, 557
- Jorgensen, I., Franx, M., & Kjaergaard, P. 1996, MNRAS, 280, 167
- Kauffmann, G. & Charlot, S., 1998, MNRAS, 294, 705
- Kauffmann, G. 1996 MNRAS, 281, 487
- Kauffmann, G., Charlot, S., & White, S. 1996 MNRAS, 283, 117

- Kauffman, G., White, S., & Guiderdoni, B. 1993 MNRAS, 264, 201
- Kelson, D., van Dokkum, P., Franx, M., Illingworth, G., Fabricant, D. 1997 ApJ, 478, 13
- Kennicutt, R. 1992 ApJ388, 310
- Kennicutt, R. 1998 astro-ph/9807187
- Kent, S. 1985 ApJS59, 115
- Kodaira, K., Watanabe, M., & Okamura, S. 1986, ApJS, 62, 703
- Kodama, T., Bower, R., & Bell, E. 1998 astro-ph 9810138
- Kormendy, J. 1977, ApJ, 218, 333
- van der Kruit, P. 1987 A&A173,59
- Larson, R. 1975, MNRAS173, 671
- Le Fèvre, O., Abraham, R., Lilly, S., Ellis, R., Schade, D., Tresse, L., Colless, M., Crampton, D., Glazebrook, K., Hammer, F., & Broadhurst, T. 1999, MNRAS submitted.
- Lilly, S.J., Tresse, L., Hammer, F., Crampton, D. & Le Fèvre, O. 1995, ApJ, 455, 108
- Lilly, S.J., Le Fèvre, O., Crampton, D., Tresse, L., 1995 ApJ, 455, 50
- Lilly, S., Schade, D., Ellis, R., Le Fèvre, O. et al. 1998 ApJ500, 75
- López-Cruz, O. 1996, PhD Thesis, University of Toronto
- Marzke, R., Da Costa, L., Pellegrini, P., Willmer, N., & Geller, M. 1998, ApJ, 503, 617
- Marzke, R., Geller, M., Huchra, J., & Corwin, H. 1994 AJ, 108, 437
- Menanteau, F., Ellis, R., Abraham, R., Barger, A., & Cowie, L. 1998 astro-ph/9811465
- Mihalas, D., & Binney, J. 1981 in *Galactic Astronomy*, San Francisco, W.H. Freeman and Company, p. 189
- Miller, G., & Scalo, J. 1979, ApJS41, 513
- Mobasher, B. & James, P. 1996, MNRAS, 280, 902
- Negroponete, J. & White, S. 1983, MNRAS, 205, 1009
- Oke, J., Gunn, J., & Hoessel, J. 1996, AJ, 111, 29
- Patton, D., Pritchet, C., Yee, H., Ellingson, E., & Carlberg, R. 1997, ApJ, 475, 29
- Pahre, M., Djorgovski, S., & de Carvalho, R. 1998, AJ, 116, 1606
- Pahre, M., Djorgovski, S., & de Carvalho, R. 1996, ApJ, 456, 79
- Press, W.H., Teukolsky, S.A., Vetterling, W.T., & Flannery, B.P. 1992, Numerical Recipes (Cambridge University Press: Cambridge)
- Rakos, K., & Schombert, J. 1995, ApJ, 439, 47
- Salpeter, E. 1955, ApJ, 121, 161
- Scalo, J. 1986 Fund. Cosmic Phys. 11, 1
- Sandage, A. & Visvanathan, N. 1978 ApJ, 225, 742
- Schade, D., Barrientos, L. F., & López-Cruz, O. 1997 ApJ477, 17
- Schade, D., Carlberg, R., Yee, H., López-Cruz, O., & Ellingson, E. 1996a, ApJ, 464, 63
- Schade, D., Lilly, S., Crampton, D., Le Fèvre, O., Hammer, F., & Tresse, L. 1995, ApJ, 451, 1
- Schombert, J. & Bothun, G. 1987 AJ, 92, 60
- Schmidt, M. 1968 ApJ, 151, 393
- Schweizer, F., & Seitzer, P. 1992 AJ104, 1039
- Silva, D. & Bothun, G. 1998a ApJ, 116, 85
- Silva, D. & Bothun, G. 1998b AJ, 116, 2793
- Simien, F. & de Vaucouleurs, G. 1986, ApJ, 302, 564
- Stanford, S.A., Peter R. Eisenhardt, P., & Dickinson, M. 1998 ApJ492, 461
- Stetson, P.B., 1987, PASP, 99, 191
- Tinsley, B. 1972, ApJ, 178, 319
- de Vaucouleurs, G. 1948, Ann. d'Astrophys. 11, 247
- White, S. & Rees, M. 1978, MNRAS, 183, 341
- Whitmore, B. 1995 *Photometry with the WFPC2* available on Space Telescope Science Institute WWW pages.
- Yee, H.K.C. 1991, PASP, 103, 396
- Zepf, S., 1997 Nature, 390, 377
- Zepf, S., & Koo, D., 1989 ApJ, 337, 34

This 2-column preprint was prepared with the AAS L^AT_EX macros v4.0.

Figure Captions

Fig. 1.— Differences in best-fit parameters from multiple observations of galaxies. The bottom panel shows the fractional bulge luminosity, B/T , in the center is the total magnitude, and on the top is the index of asymmetry. In the bottom and center panels, filled circles represent symmetric, or morphologically normal galaxies whereas open circles show asymmetric galaxies. The B/T value is not considered a valid classification index for asymmetric galaxies. The errors in a single measurement (for symmetric galaxies) as inferred from these duplicate measurements are shown on each panel. The right-most panel indicates the cut-off in asymmetry index adopted here (solid line) and in Schade et al. (1995).

Fig. 2.— Differences in structural parameters from multiple observations. Filled symbols represent symmetric (normal) galaxies and open symbols indicate asymmetric galaxies. The values of σ (computed excluding asymmetric galaxies) are shown as inferred for a single measurement from the analysis of these duplicate fits.

Fig. 3.— The relation between $M_B(AB)$ and \log of the half-light radius ($\log R_e$) for elliptical galaxies in three slices of redshift for field galaxies in the CFRS/LDSS survey. The dashed line in each panels corresponds to the best-fit to the local sequence and the solid lines indicate the best-fit *fixed-slope* ($\Delta M_B/\Delta \log R_e = -3.33$) relation for each slice. In all cases the solid lines are the best-fits with all points included. Open symbols are “discrepant” galaxies defined as those objects where visual classification gives a type earlier than S0 in apparent conflict with the class E derived by profile fitting. Spectroscopic failures (galaxies without spectroscopic redshifts) are plotted as stars at their photometrically-estimated redshifts and their trajectories as a function of redshift are indicated by light dashed lines. Large open circles indicate galaxies which have measurable [OII] emission lines. There is no clear indication that any of these sub-classes (“discrepant”, [OII]-emission, spectroscopic failures) is responsible for the shift in the mean $M_B(AB) - \log R_e$ locus.

Fig. 4.— The color-luminosity relations for elliptical galaxies in three redshift slices. Dashed lines denote the Coma relation derived from Bower, Lucey, & Ellis (1992) and the solid lines are the best-fit relations (derived holding the slope of the relation fixed at the Coma value) for the CFRS galaxies. Symbols and loci are as defined for figure 3. As in figure 3 there is no evidence that any of the sub-classes is responsible for the evolving mean color locus. Such an effect might be difficult to detect in our small sample.

Fig. 5.— Observed colors versus redshift for the CFRS galaxies with HST imaging. Filled symbols are those galaxies classified as ellipticals and open squares indicate galaxies classified as S0's (defined here as those with fractional bulge luminosities $0.4 < B/T < 1.0$) by the fitting process. Asymmetric objects have been excluded. Spectroscopic failures are plotted as filled symbols at $z = 0$ if they have been classified as ellipticals and as open symbols at $z = 1.4$ if they are later types. The color-selection criterion defined by Kauffman, Charlot, & White 1996 (plotted as a solid line) selects only a small subset of those galaxies that are classified as ellipticals or S0's by the profile fitting process.

Fig. 6.— Same as in figure 5 except that the visual classifications of Brinchmann et al. (1998) are used instead of the classifications from the fitting procedure. Again the Kauffman, Charlot, & White 1996 selection line selects only a subset of the galaxies classified visually in Paper I as early-type galaxies.

Fig. 7.— The derived shifts in luminosity (upper panels); filled circles are field ellipticals from the present work, filled pentagons are field ellipticals from Schade et al. (1996); open circles are cluster ellipticals from Schade, Barrientos, & López-Cruz 1997, and Schade et al. (1996). Lower panels are shifts in color from the present work. The colors have been corrected to represent the evolution in color of a physical galaxy (which evolves in color *and* luminosity) rather than the evolution of the mean color relation. The solid lines represent a model consisting of a single-burst population formed at $z = 10$ and the dotted lines are models where there is an added episode of exponentially declining star formation comprised of 2.5% of the final stellar mass of the galaxy beginning at $z = 1$. The single-burst models have solar abundances and the two-component models use an abundance of 40% solar for the old population and a solar abundance for the younger population. These abundance differences are the main cause of the difference in one-component and two-component model colors at $z = 0$.

Fig. 8.— The rate of star formation per unit stellar mass in elliptical galaxies as a function of redshift. At $z = 0$ the star-formation rate is taken to be zero (Kennicutt 1998). The star-formation rate is estimated from the equivalent width of [OII] emission lines and the mass is estimated from model mass-to-light ratios at $z = 0$ and galaxy luminosities that have been corrected (to $z = 0$ values) for luminosity evolution. Galaxies without [OII] emission have been included in the mass estimates.

TABLE 1
 ELLIPTICAL GALAXIES IN THE CFRS/LDSS SURVEY

ID No.	z	$M_{AB}(B)$	$\log R_e$	$(U - V)_{0,AB}$	W(OII)
13.11924	0.281	-21.17	0.629	...	0
22.0758	0.294	-20.92	0.821	2.25	0 ± 6
03.0337	0.361	-18.99	0.505	1.80	22 ± 10
03.1031	0.422	-20.26	0.328	2.14	0 ± 17
13.12112	0.424	-19.86	0.557	...	12
22.0501	0.424	-20.90	0.539	2.14	0 ± 13
10.12525	0.435	-21.60	0.685	...	3
13.12538	0.458	-19.57	0.169	...	21
10.1255	0.467	-22.02	0.798	2.28	9 ± 9
10.1231	0.473	-20.18	0.405	2.21	46 ± 19
03.1413	0.487	-20.52	0.803	1.62	0 ± 20
14.0207	0.546	-22.32	0.588	1.93	0 ± 23
22.1037	0.550	-20.02	0.306	1.78	62 ± 40
10.1262	0.577	-20.29	0.144	2.15	0 ± 8
10.0794	0.580	-20.54	-0.096	1.36	8 ± 10
22.1279	0.594	-20.80	0.708	2.02	0 ± 32
03.1032	0.618	-21.63	0.202	1.83	15 ± 2
03.1381	0.636	-22.08	0.540	1.49	14 ± 20
14.0746	0.675	-20.75	0.535	1.79	0 ± 9
03.0560	0.697	-21.09	0.555	2.31	19 ± 10
10.1207	0.706	-20.69	0.441	2.24	48 ± 28
10.1423	0.724	-20.19	0.859	1.24	9 ± 5
14.1415	0.745	-21.69	0.657	1.78	0 ± 10
03.1384	0.785	-21.26	0.685	2.06	54 ± 11
14.1311	0.807	-22.92	0.965	1.83	0 ± 2
22.1507	0.820	-21.50	0.579	2.01	0 ± 4
22.0890	0.820	-21.50	0.747	2.01	0 ± 20
10.1209	0.841	-21.99	0.564	1.75	0 ± 12
14.1496	0.899	-21.49	0.313	0.84	54 ± 12
03.1077	0.938	-22.77	1.168	1.53	0 ± 10
14.1028	0.988	-22.15	0.546	1.67	31 ± 10
14.1028	0.988	-22.15	0.585	1.67	31 ± 10
14.0854	0.992	-22.22	0.714	1.64	0 ± 15
14.0854	0.992	-22.22	0.726	1.64	0 ± 15
Discrepant Galaxies					
13.11772	0.512	-21.72	0.885	...	63
10.1243	0.585	-20.94	0.695	2.10	0 ± 15
03.1395	0.708	-20.49	1.122	1.16	0 ± 15
14.1277	0.810	-21.90	0.665	1.32	0 ± 10
14.1356	0.831	-21.01	0.646	0.96	47 ± 15
10.1189	0.949	-21.93	0.717	2.00	0 ± 5
14.0807	0.985	-21.68	0.718	0.96	0 ± 5
Photometric redshifts					
10.1248	0.61	-21.08	0.418	0.63	...
10.1313	0.66	-20.29	0.514	1.28	...
03.0321	0.76	-20.54	0.406	2.39	...
03.1426	0.82	-21.54	1.130	2.47	...
14.0516	0.94	-21.53	0.253	1.90	...

TABLE 1—*Continued*

ID No.	z	$M_{AB}(B)$	$\log R_e$	$(U - V)_{0,AB}$	W(OII)
14.1178	0.94	-21.53	0.543	1.80	...
03.0384	0.95	-21.82	-0.090	1.57	...

NOTE.—Assumes $H_0 = 50 \text{ km sec}^{-1} \text{ Mpc}^{-1}$ and $q_0 = 0.5$. R_e is in kpc, W is equivalent width in angstroms. Discrepant galaxies are those where the visual classification is inconsistent with the best-fit B/T value.

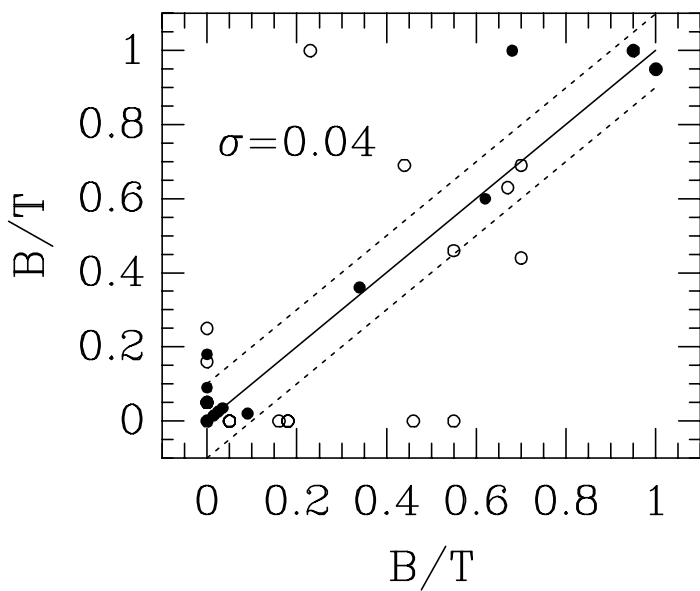
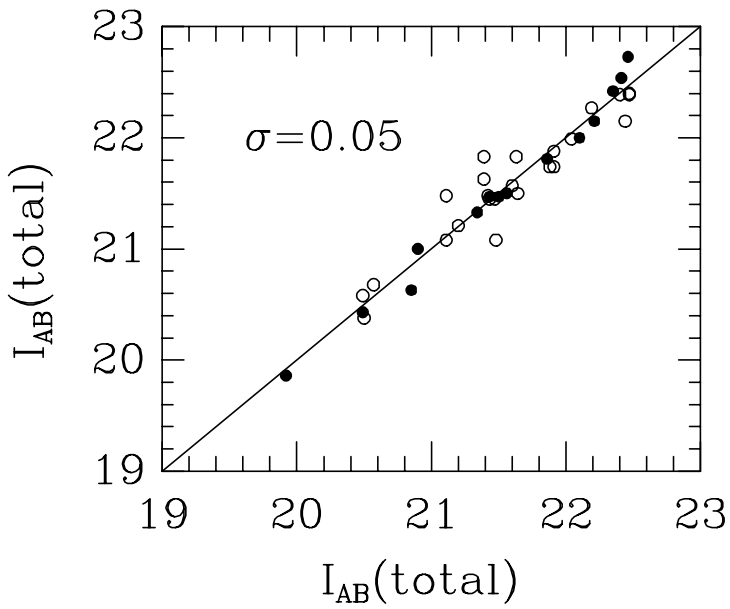
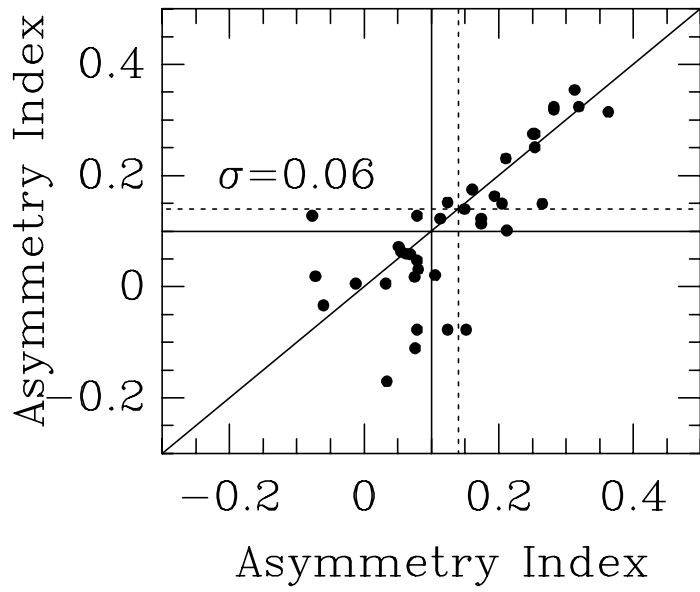


TABLE 2
SHIFTS IN THE $M_B - \log R_e$ RELATION

Sample	z	ΔM_B
All	$0.2 < z < 0.5$	0.0 ± 0.2
	$0.5 \leq z < 0.75$	-0.56 ± 0.3
	$0.75 \leq z \leq 1.0$	-0.97 ± 0.14
No Discrepant	$0.2 < z < 0.5$	\dots
	$0.5 \leq z < 0.75$	-0.85 ± 0.3
	$0.75 \leq z \leq 1.0$	-1.0 ± 0.20
No Duplicates	$0.75 \leq z \leq 1.0$	-0.90 ± 0.14

NOTE.—Assumes $H_o = 50 \text{ km sec}^{-1} \text{ Mpc}^{-1}$ and $q_o = 0.5$.

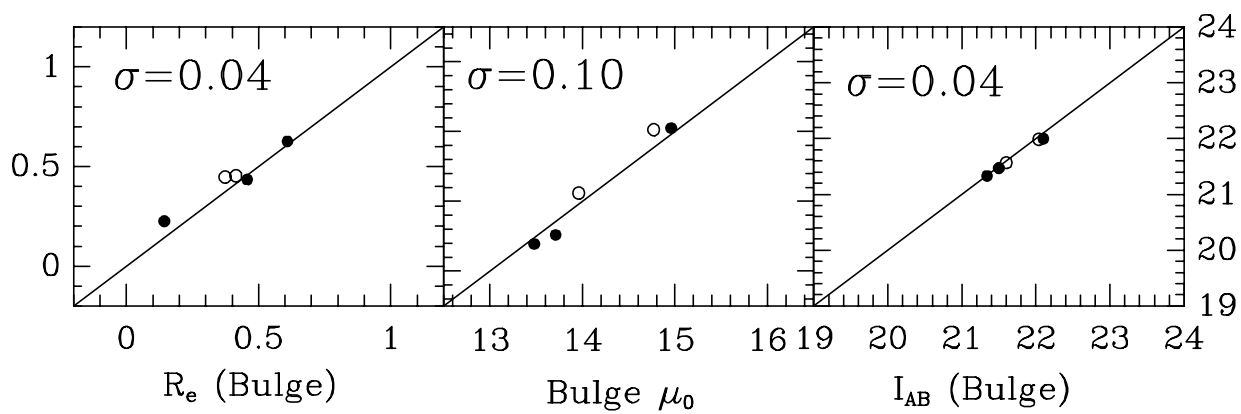
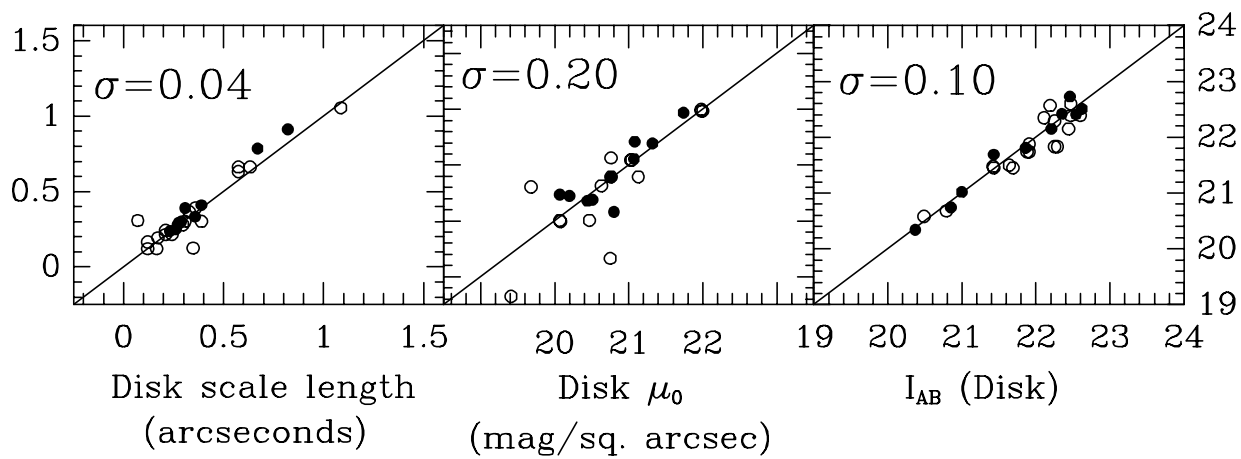
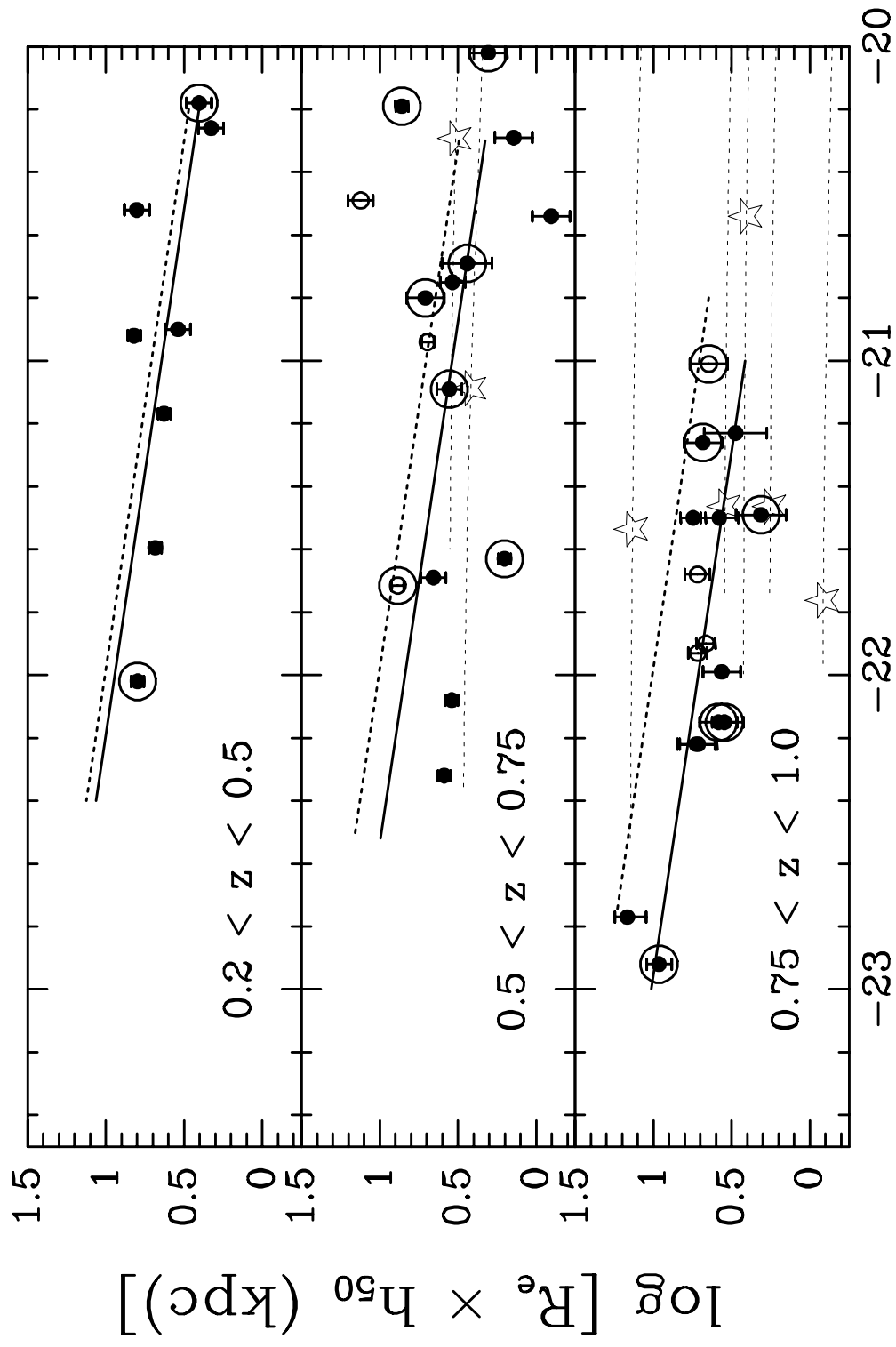


TABLE 3
OBSERVED SHIFTS IN THE $M_B - (U - V)$ RELATION

Sample	z	$\Delta(U - V)$	Intrinsic σ
All	$0.2 < z < 0.5$	-0.04 ± 0.09	0.20 ± 0.06
	$0.5 \leq z < 0.75$	-0.29 ± 0.09	0.29 ± 0.11
	$0.75 \leq z \leq 1.0$	-0.68 ± 0.11	0.29 ± 0.16
No Discrepant	$0.2 < z < 0.5$	0.03 ± 0.05	0.12 ± 0.04
	$0.5 \leq z < 0.75$	-0.30 ± 0.12	0.34 ± 0.09
	$0.75 \leq z \leq 1.0$	-0.57 ± 0.09	0.17 ± 0.19

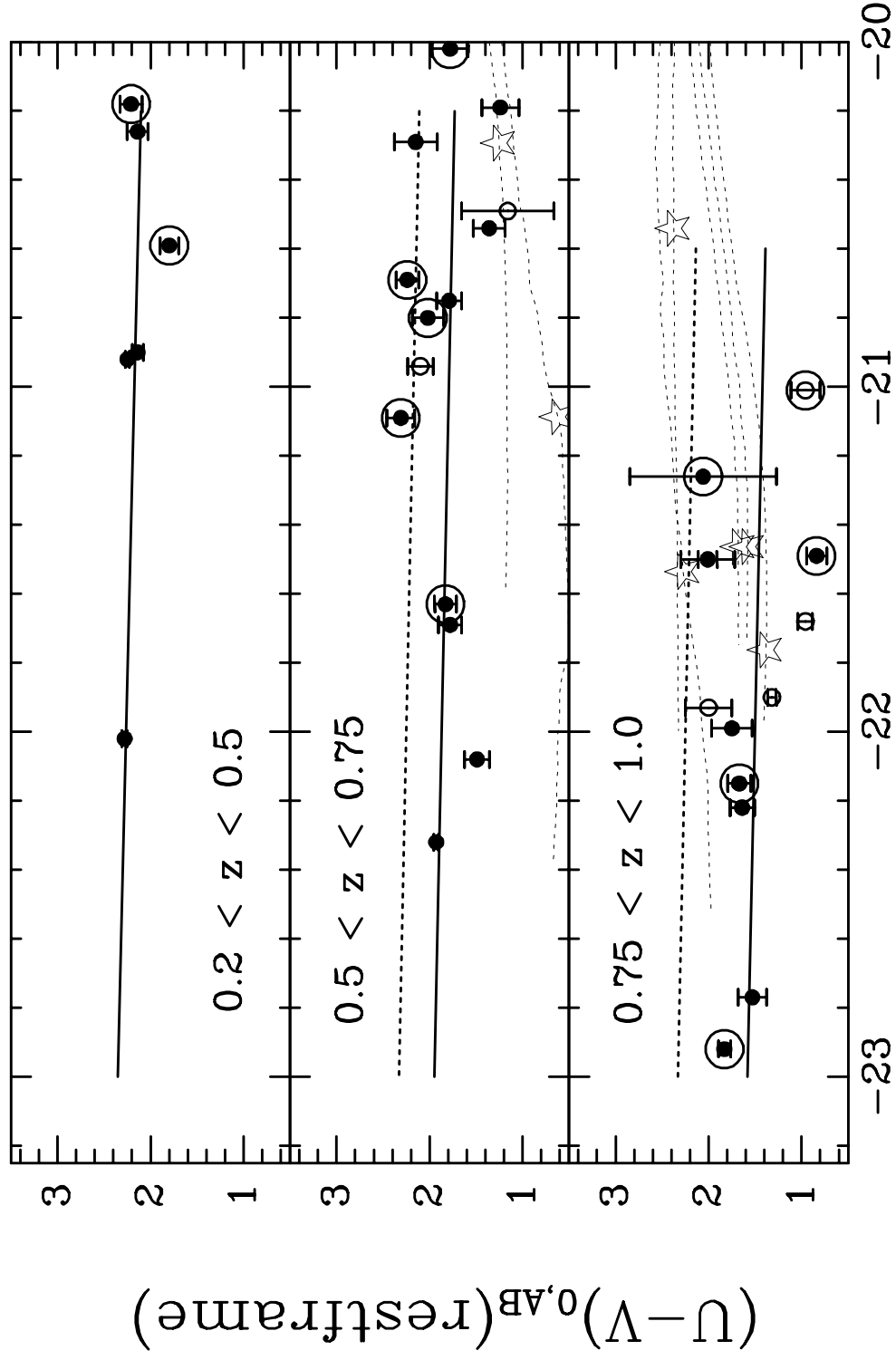


$M_B(\text{AB}) - 5 \log h_{50}$

TABLE 4
RESULTS OF THE V/V_{max} TEST

Sample	q_0	LE	$\langle V/V_{max} \rangle$	P_{ks}	γ
Sample 1	0.5	NO	0.57 ± 0.05	0.30	-2.4 [-4.0,-0.8]
Sample 1	0.01	NO	0.54 ± 0.05	0.50	-1.5 [-2.9,0.1]
Sample 1	0.5	YES	0.55 ± 0.05	0.42	-1.5 [-3.1,-0.1]
Sample 1	0.01	YES	0.52 ± 0.05	0.86	-0.7 [-2.3,0.8]
Sample 2	0.5	NO	0.61 ± 0.05	0.07	-3.9 [-5.7,-2.3]
Sample 2	0.01	NO	0.58 ± 0.05	0.20	-3.1 [-5.0,-1.5]
Sample 2	0.5	YES	0.59 ± 0.05	0.12	-2.9 [-4.5,-1.4]
Sample 2	0.01	YES	0.56 ± 0.05	0.57	-2.1 [-3.8,-0.6]
Sample 3	0.5	NO	0.47 ± 0.05	0.18	0.7 [-0.9,2.3]
Sample 3	0.01	NO	0.45 ± 0.05	0.18	1.7 [0.0,3.3]
Sample 3	0.5	YES	0.46 ± 0.05	0.18	1.3 [-0.1,2.8]
Sample 3	0.01	YES	0.43 ± 0.05	0.18	2.2 [0.7,3.8]
Sample 4	0.5	NO	0.59 ± 0.06	0.09	-3.0 [-5.0,-1.2]
Sample 4	0.01	NO	0.56 ± 0.06	0.13	-2.2 [-4.3,-0.4]
Sample 4	0.5	YES	0.58 ± 0.06	0.19	-2.1 [-3.9,-0.4]
Sample 4	0.01	YES	0.54 ± 0.06	0.36	-1.3 [-3.2,0.5]
Sample 5	0.5	NO	0.49 ± 0.04	0.75	0.1 [-1.2,1.2]
Sample 5	0.01	NO	0.47 ± 0.04	0.36	0.9 [-0.4,2.1]
Sample 5	0.5	YES	0.47 ± 0.04	0.50	1.7 [-0.5,2.9]
Sample 5	0.01	YES	0.44 ± 0.04	0.19	1.7 [0.5,2.8]
Sample 6 (Vis)	0.5	NO	0.45 ± 0.04	0.16	1.2 [0.10,2.4]
Sample 6 (Vis)	0.01	NO	0.43 ± 0.04	0.05	2.0 [0.8,3.2]
Sample 6 (Vis)	0.5	YES	0.43 ± 0.04	0.16	2.0 [0.9,3.0]
Sample 6 (Vis)	0.01	YES	0.40 ± 0.04	0.03	2.8 [1.7,4.4]
Sample 7 (Vis)	0.5	NO	0.48 ± 0.04	0.60	0.2 [-1.0,1.5]
Sample 7 (Vis)	0.01	NO	0.46 ± 0.04	0.21	1.1 [-0.2,2.3]
Sample 7 (Vis)	0.5	YES	0.46 ± 0.04	0.52	1.0 [0.0,2.2]
Sample 7 (Vis)	0.01	YES	0.44 ± 0.04	0.24	1.9 [0.7,3.1]

NOTE.—Sample 1 is composed of all elliptical galaxies (as judged from profile fitting) with spectroscopic redshifts. Sample 2 adds photometric redshifts to Sample 1. Sample 3 is Sample 1 plus spectroscopic failures but each failure is assigned a redshift of $z = 0.2$. Sample 4 is composed of Sample 1 objects but excluding “possible” S0 galaxies. Sample 5 adds all S0 galaxies (as judged from profile fitting) to Sample 1. Sample 6 is based solely on visual classifications from Brinchmann et al. 1998 and Sample 7 adds photometric redshifts. P_{ks} is the probability, calculated using a Kolmogorov-Smirnov test, that a model without number density evolution is acceptable. The best-fit exponent γ [and its 1σ confidence interval] is given for an evolutionary law of the form $F \propto (1+z)^{-\gamma}$.

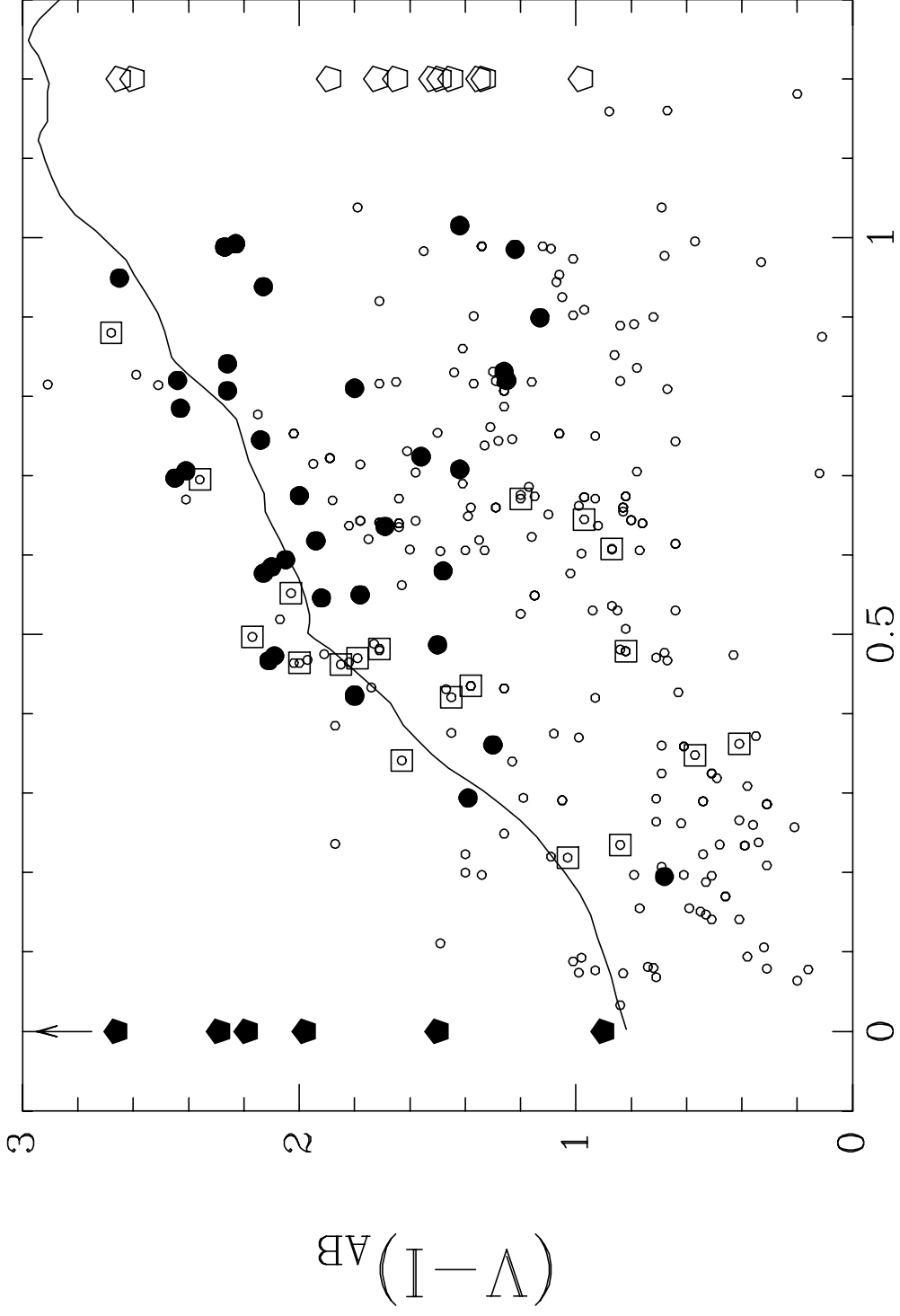


$M_B(\text{AB}) - 5 \log h_{50}$

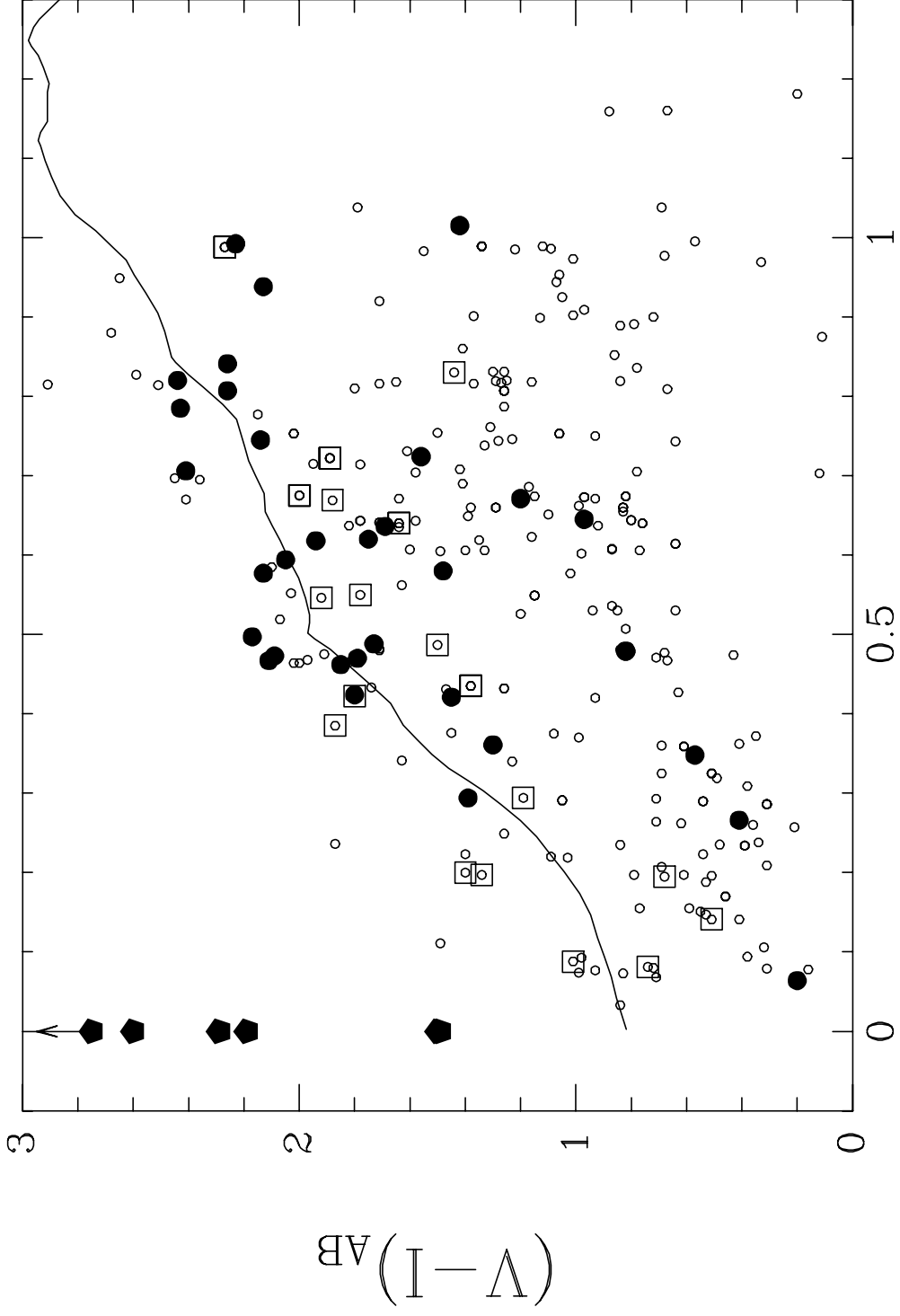
TABLE 5
COMPARISON OF PREDICTED AND OBSERVED SPACE DENSITY OF ELLIPTICALS

Redshift	Predicted $q_o = 0.5$	Predicted $q_o = 0.01$	Observed
$0.20 < z < 0.50$	3.2	4.5	5
$0.50 \leq z < 0.75$	4.9	8.4	11 (14)
$0.75 \leq z \leq 1.00$	6.2	12.8	11 (16)

NOTE.—The E/S0 LF of Marzke et al. (1998) was used to compute the space densities shown here. The numbers in parentheses include photometric redshifts.



Redshift



Redshift

